NTNU – Trondheim
Norwegian University of
Science and Technology

Undervannsovervåking ved hjelp av fiberoptisk hydrofon

Underwater surveillance using a fiber optic hydrophone

Joachim Grønhaug

Electronics System Design and Innovation
Submission date: June 2014
Supervisor: Dag Roar Hjelme, IET
Co-supervisor: Arne Løvik, Kongsberg Defence & Aerospace AS

Norwegian University of Science and Technology
Department of Electronics and Telecommunications

Problem Description

In underwater surveillance systems used in harbours and coastal areas, SONARs are used for active and passive detection of divers, small sea vehicles, speed boats and jet skis. The most common tool when using passive detection is a hydrophone cable. These cables demand electronic-to-signal conditioning and data transmission over long distances. By using a passive fiber optic hydrophone cable one can interrogate this by land without the need for underwater electronics. The assignment will be theoretical. A literature study will be performed to determine the status, potential and limits of fibre optic hydrophones. The assignment can have several approaches, such as:

- Analysis of techniques used today
- Evaluate methods for increasing the sensitivity without changing the diameter of the sensor
- Look at the possibility to make antennas with a large number of hydrophones

Abstract

Since the 1970s fiber optics has been introduced as a replacement in many industrial areas, especially in the field of communications. Another field which has been and is greatly researched is the use of fiber optic cables in sensing of temperature, strain and acoustic pressure. The common sensor for the detection of acoustic pressure under water is the piezoelectric hydrophone, however the use of an optical fiber as the sensor can provide benefits over the piezoelectric type. No electric currents underwater, resistance to electromagnetic interference, small geometries and light weight are only some of the benefits.

This thesis have emphasized on single mode fibers. A lot of theory have been provided and it has been shown that fiber optic hydrophones are highly realizable. A theoretical sensitivity of -343 dB re μPa^{-1} was calculated for a bare silica fiber. Improvements in the sensitivity were calculated for a fiber wounded around a mandrel.

The use of wavelength division multiplexing have shown that arrays consisting of many sensor heads can be used. The key role that a fiber Bragg grating has in an optical system have been discussed in terms of reflections and losses. For a high value of sensor heads, amplification is needed.

Sammendrag

Fiber optikk har blitt foreslått som en erstatning innenfor mange insdustrielle områder helt siden 1970-tallet. Dette gjelder spesielt innenfor kommunikasjon. Et annet felt som har vært og er forsket mye på, er bruken av fiberoptiske kabler som sensorer for temperatur, deformasjon og akustisk trykk. En vanlig sensor for deteksjon av av akustisk trykk under vann er den piezolektriske hydrofonen. Det er tenkt at denne kan byttes ut med en fiberoptisk hydrofon for skape fordeler denne ikke innehar. Fiberoptiske hydrofoner bruker ikke strøm under vann og er skjermet mot elektromagnetisk stråling. I tillegg er geometrien liten.

Denne oppgaven har fokuser på single mode fibere og har ved hjelp av mye teori vist at konseptet er realiserbart. En teoretisk sensitivitet på -343 dB re μPa^{-1} er beregnet. Forbedringer er kalkulert ved hjelp av en mandrel.

Bruken av bølgelengde multipleksing har vist at lange arrays med mange sensorer kan brukes. Fiber Bragg gitteres viktighet er også diskuter. For mange sensorer trengs det forsterkning i fiberen.

Preface

"With stout hearts, and with enthusiasm for the contest, let us go forward to victory."
- Bernard Montgomery

This master thesis was written as the final project of the M.Sc. program in electronics at the Norwegian University of Science and Technology. The problem description was given by Kongsberg as an introductory study on how fiber optic cables could be used as hydrophones. This thesis was carried out during the spring of 2014.

In the beginning of the project I had to use a lot of time on understanding the theory behind fiber optic hydrophones since they combine many different scientific fields. Another time consumer was also to draw all the figures and components for the fiber optic systems which I did not find any good software for. However, I am happy to have chosen this assignment as it has given me an understanding of fiber optic theory far beyond what I already knew.

I would like to thank my supervisor professor Dag Roar Hjelme for his guidance and good advice. I would also raise a thanks to Arne Løvik at Kongsberg for providing me with relevant articles and specifications for a hydrophone system which set me on the right approach for solving the problems that were given.

Trondheim, *Joachim Grønhaug*
16. juni 2014

Contents

List of Figures

Abbreviations

CW	**C**ontinuous **w**ave
DBR	**D**istributed **B**ragg **r**eflectors
DFB-FL	**D**istributed **f**eed**b**ack **f**ibre **l**aser
EM	**E**lecro**m**agnetic
FBG	**F**iber **B**ragg **g**rating
FDM	**F**requency-**d**ivision **m**ultiplexing
FWHM	**F**ull **W**idth at **H**alf **M**aximum
MM	**M**ulti **m**ode
PCF	**P**hotonic **c**rystal **f**iber
PMMA	**P**oly **m**ethyl **m**eth**a**crylate
RIN	**R**elative-**I**ntensity-**N**oise
SDM	**S**pace-**d**ivision **m**ultiplexing
SM	**S**ingle **m**ode
SNR	**S**ignal-to-**n**oise **r**atio
TDM	**T**ime-**d**ivision **m**ultiplexing
TE	**T**ransversal **E**lectric
TIR	**T**otal **I**nternal **R**eflection
TM	**T**ransversal **M**agnetic

Physical Constants

Speed of light in vacuum	c_0	$\approx$	$3 \times 10^8 \ \frac{m}{s}$
Permittivity in vacuum	ε_0	$=$	$8.854 \times 10^{-12} \frac{F}{m}$
Planck's constant	h	$=$	$6.626 \ \times 10^{-34} \ \frac{J}{s}$

Symbols

Electromagnetism

$\boldsymbol{\mathcal{E}}$	Electric field	$\frac{V}{m}$
$\boldsymbol{\mathcal{H}}$	Magnetizing field	$\frac{A}{m}$
$\boldsymbol{\mathcal{B}}$	Magnetic field	$\frac{N}{Am}$
$\boldsymbol{\mathcal{D}}$	Electric displacement field	$\frac{V}{m}$
$\boldsymbol{\mathcal{M}}$	Magnetization	$\frac{N}{Am}$
$\boldsymbol{\mathcal{P}}$	Polarization density	$\frac{V}{m}$
$\boldsymbol{\mathcal{J}}$	Current density	$\frac{A}{m^n}$
$\boldsymbol{\mathcal{S}}$	Poynting's vector	$\frac{W}{m^2}$
R	Reflectivity	
V	Fiber parameter	
M	Number of modes	
μ_r	Relative permeability	
ω	Optical angular frequency	$\frac{rad}{s}$
υ	Optical frequency	Hz
k	Optical wavenumber	$\frac{rad}{m}$
c	Speed of light in a material	$\frac{m}{s}$
λ	Optical wavelength	m
λ_B	Peak reflected Bragg wavelength	m
Λ_G	Grating period in FBG	m
I	Intensity	$\frac{W}{m^2}$
φ	Phase	
n	Refractive index	

ϵ_r	Relative permittivity	
μ_r	Relative permeability	
$\Re$	Photodetector responsivity	$\frac{A}{W}$
F	Noise factor	
NF	Noise figure	dB
Φ_{ph}	Photon flux	Photons pr second
Φ_e	Electron flux	Electrons pr second
L_c	Coherence length	m
Acoustics		
p	Pressure	Pa
Ω	Acoustic angular frequency	$\frac{rad}{s}$
f	Acoustic frequency	Hz
q	Acoustic wavenumber	Hz
Λ	Acoustic wavelength	m
v	Speed of sound in a material	$\frac{m}{s}$
S	Sensitivity	dB re μPa^{-1}
Mechanics		
ε	Strain	%
σ	Stress	Pa
E	Young's modulus	Pa
ν	Poisson's ratio	%
K	Bulk modulus	Pa
A	Area/Cross sectional area	m^2

Chapter 1

Introduction

1.1 Background

The basic building block for an underwater surveillance system is the hydrophone. Hydrophones act as transducers converting acoustic pressure into a signal. Historically, the most used hydrophone technique is the piezoelectric hydrophone. This type of hydrophone converts a pressure change generated by an acoustic source into an electric voltage by the use of a piezoelectric element. Piezoelectric hydrophones have proven to be good transducers in terms of sensitivity and are widely used. However they have some disadvantages such as the use of electric signals under water, degrading of sensitivity over time and low sustainability of high pressures/depths. In the 1970s the use of a fiber optic cable was proposed as another approach for hydrophones. Today, fiber optic cables have low cost and low loss as a result of the wide use of fiber optics in communication systems. For the the purpose of replacing the piezolectric hydrohpone the handbook of optoelectronics[5, s. 1130] lists some of the advantages of using fiber optic hydrophones:

- No electromagnetic interference(EMI)
- No short-circuiting
- Better withstanding of the corrosion in saltwater
- No electricity in the fiber optic cable and no electric circuits on the sensor itself

- Optical fiber cables are lighter, thinner and can in many cases be cheaper than electric cables
- Low loss on long distances
- Many signals can be sent on the same fiber cable
- Signals can be detected faster

In addition to the list above, fiber optic hydrophones is also said to increase both sensitivity and the dynamic range[3, s. 368] of a conventional hydrophone. The transducer principle of a fiber optic hydrophone is shown in **Figure 1.1**.

Figure 1.1: Transducing principle of fiber optic hydrophone. An acoustic source produces an acoustic signal. The pressure of the signal induces a strain in the fiber which alters the fiber, and therefore the light propagating in the fiber, which gives a measurable electric signal by the use of a photodetector.

1.2 Overview of thesis

Sensing acoustic waves with fiber optic cables covers several scientific fields such as material science, mechanics, acoustics, signal processing and electromagnetics, and it is impossible to go in depth of all the fields. This thesis will try to include most of the theory, but some fields be let out, such as nonlinearities in fibers an interferometric noise. A great amount of theory will be given and should provide the reader with a good understanding of how a fiber optic hydrophone system can be designed. It should be noted that not all of the provided theory will be used for calculation, but it will be used in the discussion, such that it can be used for designing a fiber optic system later.

Outline of thesis

- Chapter 2: Explain the basics of acoustic and electromagnetic wave and explain the continuum mechanics that models materials
- Chapter 3: Provide an insight in the field of fiber optics

- Chapter 4: Describe the basics of hydrophones in general and give the sufficient knowledge on how fiber optic sensor heads and systems can be designed
- Chapter 5: Designing fiber optic sensor heads and hydrophone systems
- Chapter 6: Discussion around fiber optic hydrophones and systems
- Chapter 7: Conclusion and future work

Chapter 2

Wave theory and continuum mechanics

When working with and designing fiber optic sensor systems it is crucial to understand the background theory of waves, both electromagnetic and acoustic, and how materials interact with these waves. This chapter will give the basics of wave theory and focus on the continuum mechanics branch of material science.

2.1 Electromagnetic waves

The fundamental equations for electromagnetic(EM) waves are Maxwell's equations, which are a set of four equations relating the electric and magnetic fields, how they can be altered and how charges and currents modify the different EM fields. These equations are usually written on differential form as seen in equation set (2.1).

$$\nabla \times \boldsymbol{\mathcal{E}} = -\frac{\partial \boldsymbol{\mathcal{B}}}{\partial t} \tag{2.1a}$$

$$\nabla \times \boldsymbol{\mathcal{H}} = \boldsymbol{\mathcal{J}} + \frac{\partial \boldsymbol{\mathcal{D}}}{\partial t} \tag{2.1b}$$

$$\nabla \cdot \boldsymbol{\mathcal{D}} = \rho_f \tag{2.1c}$$

$$\nabla \cdot \boldsymbol{\mathcal{B}} = 0 \tag{2.1d}$$

Here, $\boldsymbol{\mathcal{E}}$ is the electric field, $\boldsymbol{\mathcal{B}}$ is the magnetic field, $\boldsymbol{\mathcal{H}}$ is the magnetizing field, $\boldsymbol{\mathcal{D}}$ is the electric displacement field, $\boldsymbol{\mathcal{J}}$ is the current density and ρ_f is the free charges/total charge density.

In addition to Maxwell's equation there is a set of constitutive relations, shown in equation set (2.2), relating the electric and magnetic fields in Maxwell's equations.

$$\boldsymbol{\mathcal{D}} = \epsilon\boldsymbol{\mathcal{E}} = \epsilon_0\boldsymbol{\mathcal{E}} + \boldsymbol{\mathcal{P}} \tag{2.2a}$$

$$\boldsymbol{\mathcal{B}} = \mu\boldsymbol{\mathcal{H}} = \mu_0[\boldsymbol{\mathcal{H}} + \boldsymbol{\mathcal{M}}] \tag{2.2b}$$

In the constitutive relations ϵ is the electric permittivity, μ is the magnetic permeability, $\boldsymbol{\mathcal{P}}$ is the polarization density and $\boldsymbol{\mathcal{M}}$ is the magnetization.

Combining Maxwell's equations and the constitutive relations, and applying vector calculus, the wave equation for non-magnetic($\mathcal{M} = 0$) material without currents($\mathcal{J} = 0$) becomes

$$\nabla^2\boldsymbol{\mathcal{E}} - \frac{1}{c^2}\frac{\partial^2\boldsymbol{\mathcal{E}}}{\partial t^2} = 0 \tag{2.3}$$

where c is the speed of the electromagnetic wave, related to the permittivity and permeability of the medium by $c = (\epsilon\mu)^{-1/2}$. For a plane wave travelling in the x-direction, the wave equation(2.3) has a general solution in the form of $\boldsymbol{\mathcal{E}}(x,t) = E_0 e^{j(\omega t - kx)}$, where E_0 is the amplitude, j is the imaginary unit, ω is the angular frequency, k is the wavenumber and x is the position. The wavenumber and angular frequency are directly related to the speed, c, frequency, υ, and the wavelength, λ, of the wave as seen in equation (2.4).

$$k = \frac{2\pi}{\lambda} = \frac{\omega}{c} = \frac{2\pi\upsilon}{c} \tag{2.4}$$

The velocity, c, and the wavelength, λ, of the wave are dependent on the refractive index, n, of the medium. The refractive index of a medium is directly related to the permittivity and the permeability of the medium by $n = \sqrt{\epsilon_r\mu_r}$, where $\epsilon_r = \frac{\epsilon}{\epsilon 0}$ is

the relative permittivity and $\mu_r = \frac{\mu}{\mu_0}$ is the relative permeability of the medium. Dielectrics are usually non-magnetic, meaning $\mu_r = 1$, such that the refractive index can be written as

$$n = \sqrt{\epsilon_r}. \tag{2.5}$$

Air has a refractive index of $n \approx 1$ such that the electromagnetic wave will travel at the speed of light in vaccum, $c_0 = 3 \cdot 10^8 \frac{m}{s}$. For materials with other refractive indices, the speed of light will change by the relation $c = \frac{c_0}{n}$ and the wavelength will change by $\lambda = \frac{\lambda_0}{n}$, where c_0 and λ_0 are the values in vacuum.

After establishing the basic equations for electromagnetic waves, the intensity, I, of the wave can be found by time-averaging the Poynting's vector, $\boldsymbol{\mathcal{S}} = \boldsymbol{\mathcal{E}} \times \boldsymbol{\mathcal{H}}$, which gives the expression for the intensity as

$$I = \langle \boldsymbol{\mathcal{S}} \rangle = \frac{1}{2} \mathrm{Re}(\boldsymbol{\mathcal{E}} \times \boldsymbol{\mathcal{H}}^*) \tag{2.6}$$

where $\langle \boldsymbol{\mathcal{S}} \rangle$ is the time averaged root mean square value of the Poynting's vector, $\boldsymbol{\mathcal{S}}$ and $\boldsymbol{\mathcal{H}}^*$ is the complex conjugate of the magnetic field.

2.1.1 Laser

The laser is one of the most important scientific discoveries of the 20th century. Lasers can be based on both gas, solids and liquids. Different materials and setups are used dependent on the desired wavelength which is radiated, and some lasers can also be tuned between different wavelengths. It is possible to operate a laser in either continuous wave(CW) mode or pulsed, but the CW mode can be operated in pulsed mode by using an external modulator. A laser has the ability to produce nearly monochromatic light, meaning the light will have a narrow linewidth centered at a single frequency. The advantage of having monochromatic light has lead to investigation and interaction with materials in ways impossible with other light sources. This has made the laser one of the basic building blocks of optical communication systems.

A laser's ability to produce a small spectral width increases the coherence length of the light. The coherence length, L_c, describes the distance, a wave will maintain a degree of coherence and can be found from

$$L_c \approx \frac{\lambda^2}{\Delta\lambda} \tag{2.7}$$

where λ is the central frequency. For the frequency domain the coherence length is found from

$$L_c \approx \frac{c}{\Delta\nu} \tag{2.8}$$

where $\Delta\nu$ is the spectral linewidth of the laser.

Lasers are also sources of noise of an optical signal. Two common sources are the relative intensity noise(RIN) and phase noise[6]. RIN arises from the fluctuations of the output power of the laser, and is relative to the average power lever radiated from the laser. RIN are

2.1.2 Interference and interferometry

Using a laser with a narrow spectral width gives rise to the use of interferometry, meaning the interaction between equally polarized monochromatic waves at a point. The limitation lies in the coherence length such that the path length between the two waves must be shorter than the coherence length of the laser. At a given point in space the two waves can be added together by the principle of superposition. This will create a new wave which will have its intensity as a function of the phase difference between the two waves. To show this, it is necessary to start out with two monochromatic($\omega = \omega_1 = \omega_2$) waves with different phases(φ_1, φ_2), with $U_1 = e^{j(\omega t - \varphi_1)}$ and $U_2 = e^{j(\omega t - \varphi_2)}$. At an interfering point the sum of the two waves can be written[1, p. 58]

$$U(\mathbf{r}) = U_1(\mathbf{r}) + U_2(\mathbf{r}) \tag{2.9}$$

For simplification, the amplitude of a wave is written as[1, p. 58] $I_n = |U_n|^2$. The intensity at the interfering point then becomes

$$I = |U|^2 = |U_1 + U_2|^2 = |U_1|^2 + |U_2|^2 + U_1^* U_2 + U_1 U_2^* \tag{2.10}$$

which gives the interference equation for two monochromatic waves as

$$I = I_1 + I_2 + 2\sqrt{I_1 I_2}\cos(\varphi) \tag{2.11}$$

where $\varphi = \varphi_2 - \varphi_1$.

For two waves with the same intensity($I_0 = I_1 = I_2$) the equation simplifies to

$$I = 2I_0\left[1 + \cos(\varphi)\right] \tag{2.12}$$

Interferometers can be set up in different ways, where the most used are the Mach-Zehnder, Michelson, Fabry-Perot and the Sagnac interferometer. A bulk setup for Mach-Zehnder and Michelson can be seen in **Figure 2.1** and **2.2**, respectively.

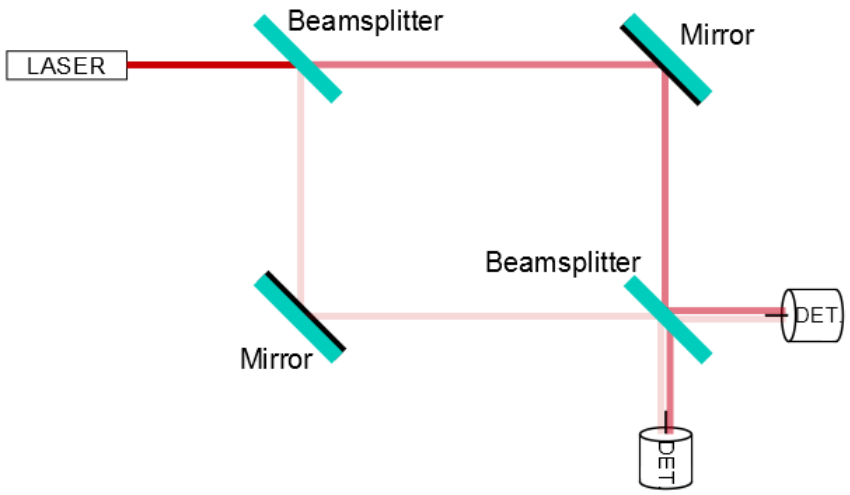

Figure 2.1: Bulk optic Mach-Zehnder interferometer. The laser beam is split into two equal waves which travel different paths. The waves then interfere in the last beam splitter and gets split into two detectors. This setup can also be used with only one detector.

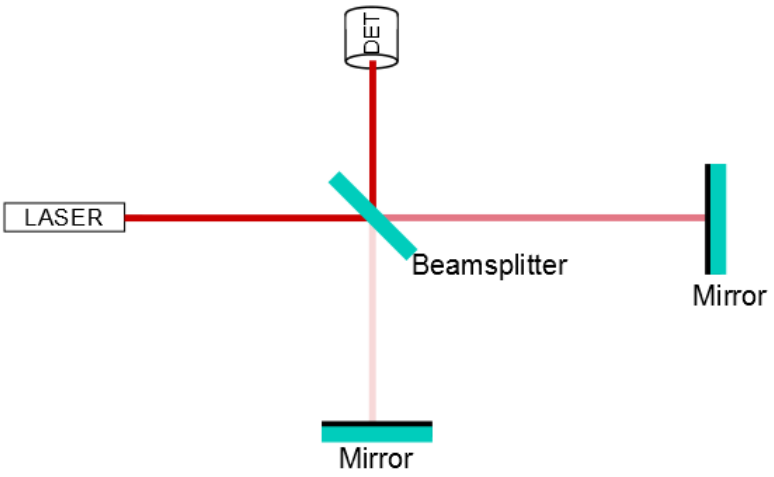

Figure 2.2: Bulk optic Michelson interferometer. The laser beam is split into two equal waves. Each wave is reflected back to the beam splitter where they interfere.

2.1.3 Polarization

The polarization is a property that describes the direction of the oscillating electromagnetic fields of a wave. For waveguides, such as a fiber optic cable, there are three operating modes:

- Transverse electromagnetic(TEM) is an electromagnetic wave having no electric and magnetic field in the propagating direction.
- Transverse electric(TE) is an electromagnetic wave having no electric field in the propagating direction.
- Transverse magnetic(TE) is an electromagnetic wave having no magnetic field in the propagating direction.

In interferometry it is crucial that the waves, which are interfering, maintains an equal polarization to create the actual interferometric result. Misaligned polarizations can create false results as shown in **Figure 2.3**. This means that the interfering waves can have the same phase, but the measured intensity of the waves is reduced according to the angle between the polarization. The worst case scenario is when two waves with equal intensity are in phase, but with fields rotated 180^0 to each other. This will create a zero intensity output, but should have produced a maximum intensity output.

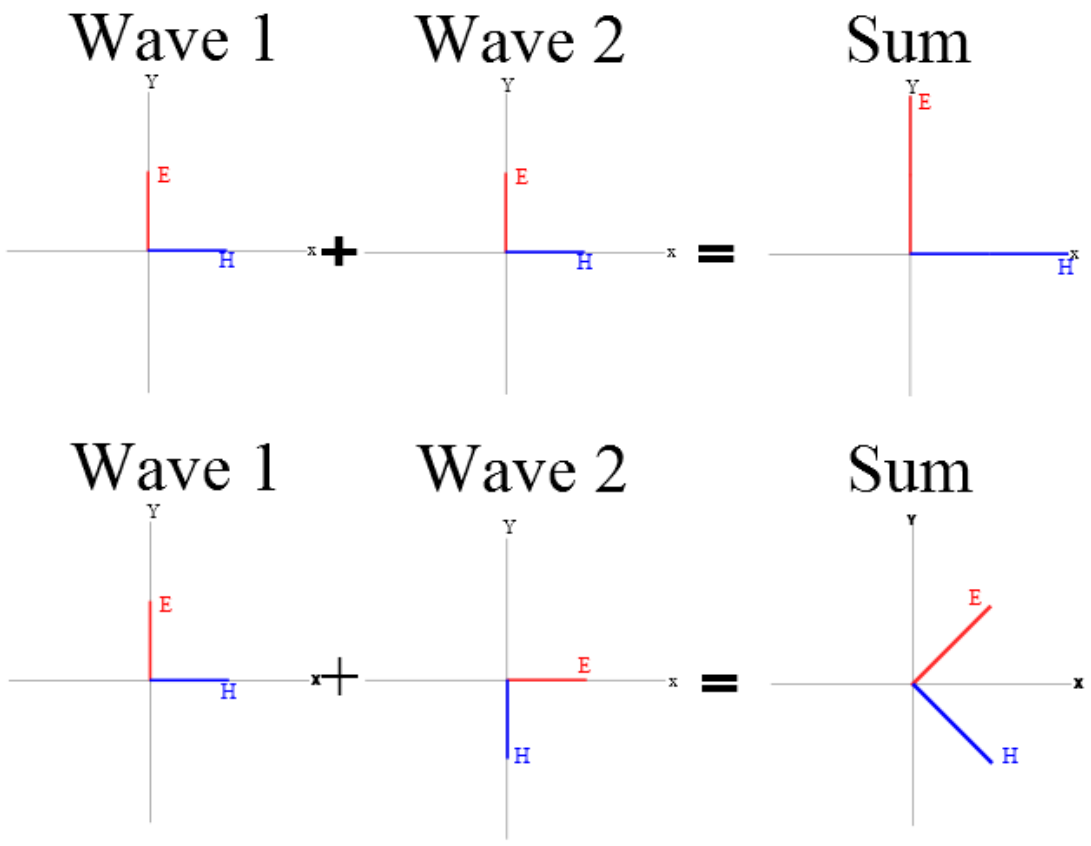

Figure 2.3: Polarization and interferometry. (top) Two waves of equal polarization and intensity are summed. (bottom) Two waves with different orientation of polarization, but with equal intensity.

2.1.4 Photodetectors

Optical detectors works as absorbers of light; converting the incoming light(photons) into electric energy. An optical wave consists of many photons, where each photon has an energy of $E_{ph} = h\upsilon$, where h is the Planck's constant. For a semiconductor photodetector the photon energy has to be larger than the bandgap of the material to excite electrons from the valence band into the conduction band. The probability of a photon to excite an electron is defined as the quantum efficiency η[1, p. 753]. The power of the wave can be written as $P = h\upsilon\Phi_{ph}$ and the short-circuit electric current as $i_{ph} = e\Phi_e$, where Φ_{ph} is the photon flux, related to the electron flux by $\Phi_e = \eta\Phi_{ph}$. This gives the relation between the incident power and the current generated as

$$i_p = \frac{\eta e P}{h\upsilon} = \Re P \tag{2.13}$$

where e is the charge of the electron and the photodetector responsivity $\Re = i_p/P$ is defined by[1, p. 754]

$$\Re = \frac{\eta e}{h\upsilon}. \tag{2.14}$$

The responsivity varies with the wavelength of the incident light because the quantum efficiency has a wavelength dependence $\eta(\lambda)$, which is a result of the spectral responses of the semiconductor material[1, p. 760].

A photodetector can operate in two modes: *photoconductive* and *photovoltaic*. For the photoconductive mode the detector is biased by an external current. The output current of the circuit is then proportional to the incident power on the detector, but will have an addition to the current known as dark current, i_d. For photovoltaic mode no bias is applied and a voltage in the circuit is measured.

2.2 Acoustic waves

The wave equation for acoustic waves takes form of a partial differential equation, as for an electromagnetic wave, but the variables are different. Whereas the electromagnetic wave equation were derived from Maxwell's equations, the acoustic wave equation arises from the ideal gas law($pV = nRT$), modelling the propagating medium as a gas, and can be shown to be

$$\nabla^2 p - \frac{1}{v^2}\frac{\partial^2 p}{\partial t^2} = 0 \tag{2.15}$$

where p is the pressure and v is the velocity of the wave.

For an acoustic plane wave travelling in the x-direction the solution to the wave equation can be written as

$$p(x,t) = p_0 \sin(\Omega t - qx) \tag{2.16}$$

where Ω is the acoustic angular frequency, q is the acoustic wavenumber and x is the position of the wave. As for the electromagnetic wavenumber, k, the acoustic

wavenumber is related to the acoustic wavelength Λ, velocity v, and frequency f by

$$q = \frac{2\pi}{\Lambda} = \frac{\Omega}{c} = \frac{2\pi f}{c} \tag{2.17}$$

The velocity is defined by $v = \sqrt{\frac{K}{\rho_0}}$, where K is the bulk modulus, which will be described in Section 2.3.3 and ρ_0 is the density of the medium. By knowing the density and bulk modulus the acoustic impedance, Z, can be found by

$$Z = \rho_0 v = \sqrt{\rho_0 K} \tag{2.18}$$

2.3 Continuum mechanics and solids

Continuum mechanics is the area of material science that deals with the motion and mechanical behavior of masses. In continuum mechanics, the material is evaluated as a mass, as opposed to a set of discrete particles. This is possible if the dimensions of the material is much greater than the interatomic distances which simplifies the equations for how a material reacts to external forces.

In solid mechanics materials are divided into elastic and non-elastic materials. For elastic materials an applied force will cause a deformation that is reversible, meaning that it will recover its original dimensions when the applied force is removed. For non-elastic materials, or for elastic materials with applied stress greater than their elastic limit, the material will be permanently deformed after an applied force is removed and therefore retain the new dimensions gained by the applied force.

2.3.1 Deformation

When explaining the physics of deformation one usually starts out with defining the stress, σ, on a material. Stress is as defined pressure per area as seen in equation (2.19) and is usually measured in pascals(Pa), where $1\text{Pa} = 1\frac{N}{m^2}$.

$$\sigma = \frac{F}{A_0} \tag{2.19}$$

In equation (2.19) F is the applied force and A_0 is the original cross sectional area where the force is exerted.

Strain is a unitless description on how a material is deformed relative to how it is changed in length in a direction. The normal strain, ε, is positive if the material is stretched and negative if it is compressed, as can be seen in equation (2.20).

$$\varepsilon = \frac{l' - l}{l} = \frac{\mathrm{d}L}{L} \tag{2.20}$$

In equation (2.20) l' is the length of a dimension in a material under applied stress and l is the original length without any applied stress. Materials can have different strains in different directions which can be described on matrix form shown in equation (2.21).

$$\varepsilon = \begin{bmatrix} \varepsilon_{xx} & \varepsilon_{xy} & \varepsilon_{xz} \\ \varepsilon_{yx} & \varepsilon_{yy} & \varepsilon_{yz} \\ \varepsilon_{zx} & \varepsilon_{zy} & \varepsilon_{zz} \end{bmatrix} \tag{2.21}$$

2.3.2 Poisson's ratio

Poisson's ratio, ν, describes how a material changes in dimensions when it is compressed or stretched in one direction. E.g. when there is a transversal strain the material can be compressed in the transversal direction, but expand in the axial direction, where the Poisson's ratio is given in equation (2.22).

$$\nu = -\frac{d\varepsilon_{\text{trans}}}{d\varepsilon_{\text{axial}}} \tag{2.22}$$

In equation (2.22) ϵ_{trans} is the transversal strain, which has a negative value if stretched and a positive value if compressed. ϵ_{axial} is the axial strain, which has a positive value when stretched and a negative value if compressed.

As for the strain, ε, Poisson's ratio can be vary with the directions of the material and can therefore be represented on matrix form as seen in equation (2.23).

$$\nu = \begin{bmatrix} \nu_{xx} & \nu_{xy} & \nu_{xz} \\ \nu_{yx} & \nu_{yy} & \nu_{yz} \\ \nu_{zx} & \nu_{zy} & \nu_{zz} \end{bmatrix} \tag{2.23}$$

2.3.3 Young's modulus and bulk modulus

One of the most common parameters for describing the mechanical properties of a material is the Young's modulus E. The Young's modulus describes the elastic properties of a material and is also known as the modulus of elasticity. It is defined as the ratio between stress and strain

$$E = \frac{\text{stress}}{\text{strain}} = \frac{\sigma}{\varepsilon}. \tag{2.24}$$

A material will experience a relative decrease in volume when it experiences a uniform pressure. The bulk modulus, K, describes how a material reacts to a surrounding uniform compression and is defined by

$$K = -V\frac{\mathrm{d}p}{\mathrm{d}V} = \rho\frac{\mathrm{d}p}{\mathrm{d}\rho} \tag{2.25}$$

where V is the volume of the material, P is the pressure and ρ is the density. For a homogeneous, linear and elastic material the bulk modulus is related to the Young's modulus, E, and the Poisson's ratio, ν, by

$$K = \frac{E}{3(1-2\nu)}. \tag{2.26}$$

An interesting fact is that for $\mu = \frac{1}{3}$ the Bulk modulus will be equal to the the Young's modulus, $K = E$.

Chapter 3

Fiber optics

This chapter will describe the operating principle of a fiber optic cable in order to to fully understand how light propagates and can be altered in a fiber. Fiber types and losses, multiplexing techniques, fiber optic interferometry, fiber Bragg gratings and dispersion in fibers are also provided to be able to design a fiber optic system.

3.1 Fiber optic theory

A fiber optic cable, with its cross section shown in figure 3.1, usually consists of:

Core A dielectric where the light travels and is confined.

Cladding A dielectric which encapsulates the core with a slightly lower refractive index than the core.

Buffer A component which isolates the core and cladding from physical damages and works as a spacing between the jacket and cladding.

Jacket The outermost layer which is usually a polymer protecting the fiber. The jacket can also be used as the buffer, becoming the outermost layer.

In addition, the fiber can also be bare(or stripped), such that it only consist of the core and cladding. The outermost layer can also consist of several layers

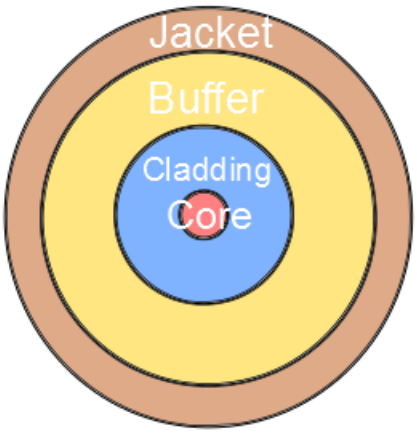

Figure 3.1: Cross section of an optical fiber with naming of layers.

with buffers and jackets to protect it from hazardous environments or improve the acoustic sensitivity of the fiber, which will be explained in Section 4.5.

The operating principle of an optical fiber arises from the phenomenon of total internal reflection(TIR). TIR allows for an electromagnetic wave to be confined inside a dielectric given that:

1. The media surrounding the dielectric has a lower refractive index.
2. The angle at which the electromagnetic wave is incident on the boundary between the two media is lower/higher than the critical angle, θ_c.
3. The angle of which light is coupled into a fiber from another media is below the acceptance angle, θ_a.

To better understand where this set of rules comes from, we start out with Snell's law, given in equation (3.1) and illustrated in **Figure 3.2**.

$$n_1 \sin\theta_1 = n_2 \sin\theta_2 \tag{3.1}$$

In equation (3.1), n_1 and θ_1, are the refractive index and incoming angle of an electromagnetic wave in medium 1 and n_2 and θ_2, is the refractive index and outgoing angle of an electromagnetic wave in medium 2. By having this relation one can e.g. determine the direction an electromagnetic wave will propagate with after passing the boundary between two media. To achieve TIR there is need to

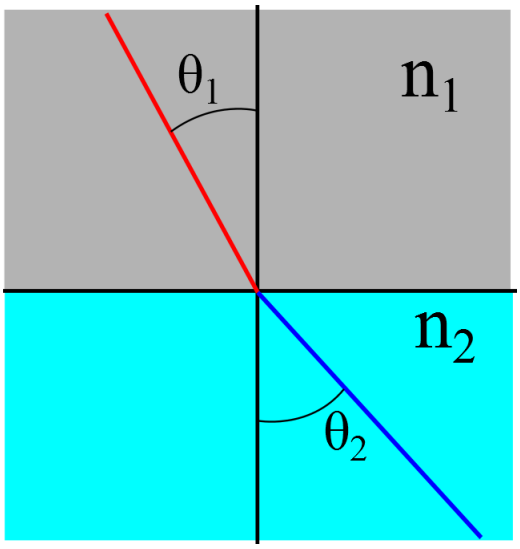

Figure 3.2: Illustration of snells law. A ray of light(red) is propagating in a medium with a refractive index n_1. When the ray crosses the boundary into a medium with a refractive index n_2 it gets refracted into an angle $theta_2$. The angle $theta_2$ can be calculated using Snell's law in equation (3.1) when all the other parameters are known.

find the angle at which the refracted ray travels along the boundary between the two media meaning $\theta_2 = 90°$ and giving $\sin(90) = 1$. This leads to the relation $\theta_1 \leq \sin^{-1}(n_2/n_1)$ which gives the definition of the critical angle, θ_c, as

$$\theta_c = \sin^{-1}\left(\frac{n_2}{n_1}\right) \tag{3.2}$$

All incoming waves at angles above the critical angle, θ_c, will then experience TIR and be reflected at the boundary between the two media, confining the wave in media 1. This is satisfied only when $n_2 < n_1$, because the $\sin^{-1}$-function is only defined for values lower than 1.

Relating the concept of TIR to the fiber optic cable we can regard the previously described media 1 as the core and media 2 as the cladding. An example of creating a difference in the refractive index of the core, n_{co}, and cladding, n_{cl}, is to use a pure silica core and dope the silica in the cladding with fluorine. This will lower the claddings refractive index. By knowing the critical angle, the acceptance angle, θ_a, can be calculated. The acceptance angle determines the maximum angle at which an electromagnetic wave can be coupled into a fiber and experience TIR, and is defined by

$$\theta_a = \sin^{-1}(\text{NA}) \tag{3.3}$$

where NA is the numerical aperture given by

$$\text{NA} = \sqrt{n_{\text{co}}^2 - n_{\text{cl}}^2} \tag{3.4}$$

The fiber cable with acceptance angle and critical angle is illustrated in **Figure ??**.

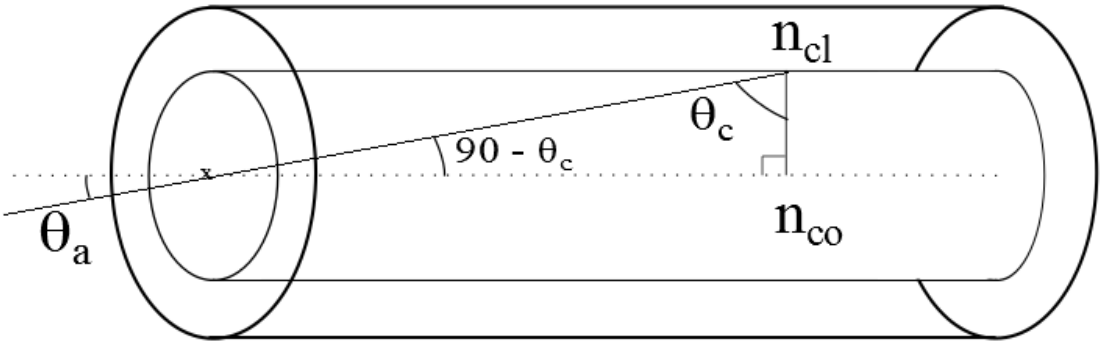

Figure 3.3: Illustration of the total internal reflection in a fiber. The critical angle θ_c determines the acceptance angle.

Having the NA, the normalized frequency(also known as the fiber parameter), V, can be defined as[1, p. 334]

$$V = 2\pi \frac{a}{\lambda_0} \text{NA} \tag{3.5}$$

where a is the radius of the fiber core. If $V < 2.405$ the fiber is single mode(SM) and for $V > 2.405$ a multi mode(MM) fiber. The value of $V = 2.405$ is the first zero of the first order Bessel function, used when solving the paraxial wave equation used for determining the wave properties of an optical fiber[1, p.336]. A mode is a solution to the paraxial wave equation and describes how many rays that can propagate in the fiber. For a normalized frequency $V < 2.405$ will only give one allowed mode for the fiber.

The propagation constant in an optical fiber is usually written as β. For weakly guiding fibers($n_{\text{co}} - n_{\text{cl}} \ll 1$) the propagation constant is directly related to the refractive index of the core and can be written as

$$\beta \approx k_0 n_{\text{co}} \tag{3.6}$$

3.2 Fiber optic interferometry

Interferometry was explained in Section 2.1.2 and illustrated by using mirrors. For optical fibers interferometry can be done by splitting the wave with a coupler into fibers and combine them with another coupler, such as in the fiber optic Mach-Zender interferometer in **Figure 3.4**. The laser is sent into a fiber which is connected to a coupler, splitting the signal into two arms. Depending on how the length in these two arms differ, and if they differ less then the coherence length, a signal can be detected. The two arms are usually called sensing and reference arms. The end coupler is arranged such that both waves can be coupled into a single sensor or into two sensor. Fiber optic setups for the other interferometry techniques described in 2.1.2 are also realizable.

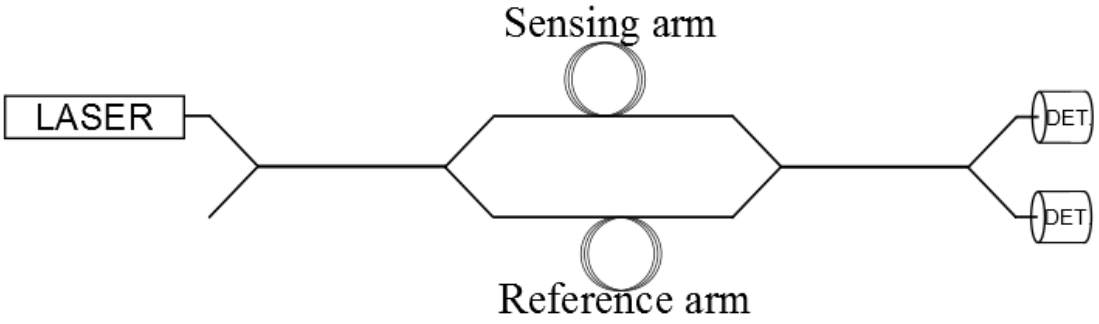

Figure 3.4: Fiber optic Mach-Zender interferometer. A laser is sent into a coupler which splits the signal into two reference arms. The output signal one the two detectors is modulated dependent on how the path difference between the two arms changes.

For interferometric configurations, there are two possible path schemes: balanced and unbalanced[3, p. 370]. The balanced scheme has approximately equal length of the reference and sensor arms, as in **Figure 3.4**, which can achieve sensing with lasers that have low coherence length. For the unbalanced scheme, the reference arm is much shorter the sensing arm. The long path difference in unbalanced schemes requires lasers with long coherence length.

3.3 Fiber types and materials

The basic principle of an optical fiber is to transmit light between the two fiber ends. Fibers can be single mode(SM) or multimode(MM) as previously described in Section 3.1, but other variants also exists such as polarization maintaining(PM) fiber and rare earth doped(active) fibers. PM fibers have the ability of maintaining the polarization throughout the fiber length which can provide beneficial for interferometric purposes described in Section 2.1.2. Active fibers can be pumped by a lower wavelength source which can amplify higher wavelengths propagating in the fiber. Common dopants are Ytterbium and Erbium which are rare earth materials.

For fiber materials, silica based fibers are the most commonly used today. They have good production techniques, low losses, low cost and can also be photosensitive such that fiber Bragg gratings can be written. These factor making them highly suitable for fiber optic systems. The confinement of light in the core is based on total internal reflection(TIR), as described earlier in the chapter. Operating wavelengths go from 400 - 1800 μm, but the most common is the 1.55 μm, which can have losses as low as 0.2 dB/Km.

An emerging field is the use plastic optical fibers, or polymer optical fibers(POFs). POFs are made out synthetic materials, where the core often consists of acrylic(REF) and the cladding some fluorinated polymer(REF). These fibers have the benefit of being inexpensive and having a high mechanical flexibility, but they are big in diameter with respect to the silica fiber and they have high attenuation[7].

Silica and polymer fibers can also be structured as photonic crystal fibers(PCFs). In a PCF the cladding is a customized geometrical structure, with an example given in **Figure 3.5**. The geometric structure forms a photonic crystal which creates photonic bandgaps, allowing for confinement of selected different wavelengths in the core. PCFs is a relatively new concept which has higher attenuation compared a silica fiber, and can experience high losses if bended. This bend losses arises from the change in geometry of the holes in the cladding. The use a of photonic crystal as a cladding allows for the core to be air, which is not possible with the TIR-based silica fiber that requires the cladding to have lower refractive index.

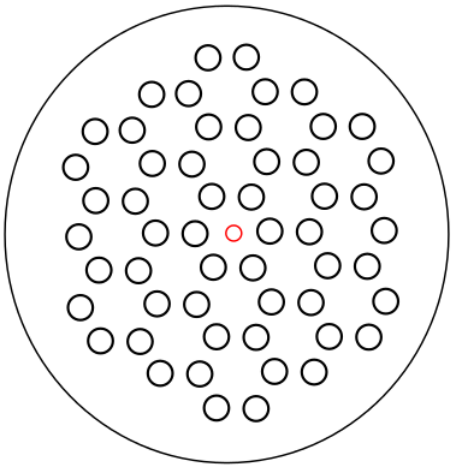

Figure 3.5: Typical cross section of a PCF[1, p. 360]. The red circle is the core and the geometric structure with black circles(holes) forms the cladding.

3.4 Multiplexing

Multiplexing is used to reduce the amount of fibers needed in a system, allowing multiple signals to propagate on one or a pair of optical fibers giving rise to the use of several sensors on a single optical fiber. For sensor uses the chosen multiplexing technique can determine not only how many sensors that can be used on a single fiber, but it can also determines the frequency response, dynamic range, cross-talk and cost effectiveness. Multiplexing techniques also have the ability to be combined to allow even more signals on a single fiber, creating systems which can support more sensors. In addition to the two multiplexing techniques that will be described below, there are also techniques such as frequency division multiplexing(FDM), space division multiplexing(SDM) and code division multiplexing(CDM). FDM and CDM will not be discussed in this thesis and SDM can be explained to be that signals are split into different cables.

3.4.1 Time division multiplexing(TDM)

In TDM the different signals are multiplexed and sent at different times such that every signal gets its own timeslot. For systems operating with bits, the bit-rate for the link between the multi- and demultiplexer has to be a multiple of the bit-rate of the channels times the channels. An example of this is shown in Figure 3.6.

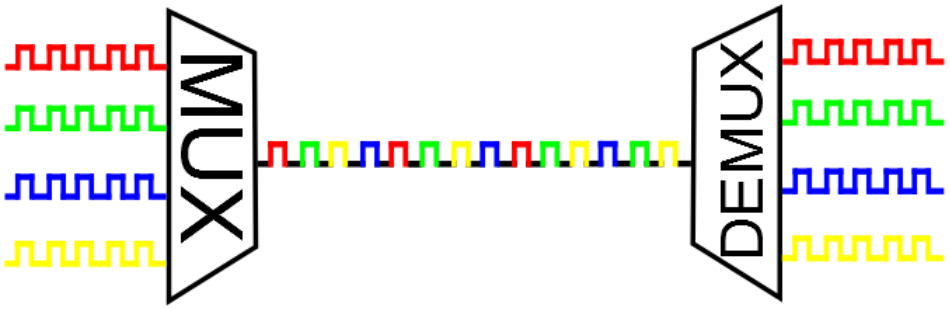

Figure 3.6: Operating principle of TDM

3.4.2 Wavelength division multiplexing (WDM)

The WDM multiplexing scheme allows for different wavelengths to propagate on a single fiber. The spectral separation of the wavelengths propagating can be both big as in coarse WDM(CWDM) or relatively small as in dense WDM(DWDM). In DWDM the frequency spacing can be as low as $\Delta\nu$ =12.5 GHz[8] which corresponds to a wavelength spacing of $\Delta\lambda = 0.1$ nm. The operating wavelengths are around 1.55 μm and standardized by the International Telecom Union(ITU) and divided into bands[8].

Figure 3.7: Operating principle of WDM. Each color represents a different wavelength. The different wavelengths are combined onto single fiber by a multiplexer and then demultiplexed onto four new fibers.

3.5 Fiber Bragg grating

A fiber Bragg grating(FBG), visualized in figure 3.8, is an optical grating consisting of alternating refractive indices in a fiber core. It plays an essential part in modern fiber optic systems and can be used in many disciplines in optics. The length of the grating period, Λ_G and the effective refractive index, n_{eff} experienced by an incoming wave determines the Bragg wavelength, λ_B. λ_B is the peak reflected

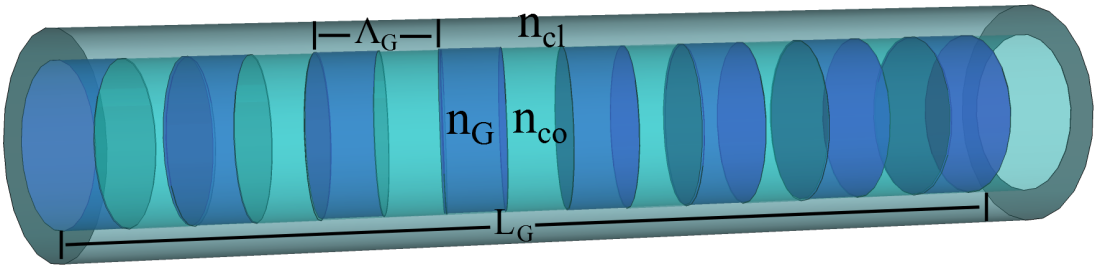

Figure 3.8: Sketch of fiber Bragg grating in an optical fiber. The change in the color of the core corresponds to a change in the refractive index.

wavelength by the grating. The amount of power that is reflected is determined by length of the grating, L_G, and the strength of the grating, $\delta n_0 = n_G - n_{co}$. The grating strength can be used to set the bandwidth, usually measured at full width half maximum(FWHM), and the grating length can be used to set the peak reflectivity. In silica fiber, the core needs to be photosensitive and radiated by UV-light to create the desired grating structure. By changing the angles, intensity and/or exposure time, one can change the grating period, grating length and the strength of the written refractive index, n_G. The general formula for the peak reflected wavelength FBG is

$$\lambda_B = 2n_{\text{eff}}\Lambda_G \tag{3.7}$$

where, for a uniform grating, the effective refractive index is found by $n_{\text{eff}} = (n_G + n_{co})/2$. And the reflectivity, R, of an FBG can be calculated from [9]

$$R = \frac{\kappa^2 \sinh^2(S_G L_G)}{\Delta\beta \sinh^2(S_G L_G) + \kappa^2 \cos 2(S_G L_G)} \tag{3.8}$$

where $\kappa = \pi\delta n_0/\lambda$ is the coupling constant, $\Delta\beta = \beta - \pi/\Lambda_G$ is the wave vector detuning, $\beta = 2\pi n_{co}/\lambda$ is the propagation constant of the fiber core and $S_G = \sqrt{\kappa^2 - \Delta\beta^2}$. The reflectivity and transmission of a theoretical FBG can be seen in **Figure 3.9**.

Figure 3.9 is drawn for illustrative purposes and a real uniform FBG will have sidelobes in its reflectivity spectrum. The stronger the FBG, the more it will reflect portions of other wavelengths, however this can be dampened by apodizing the grating[9]. For very weak(in reflectivity) gratings this is generally not a problem since the side lobes will be suppressed to a negligible level.

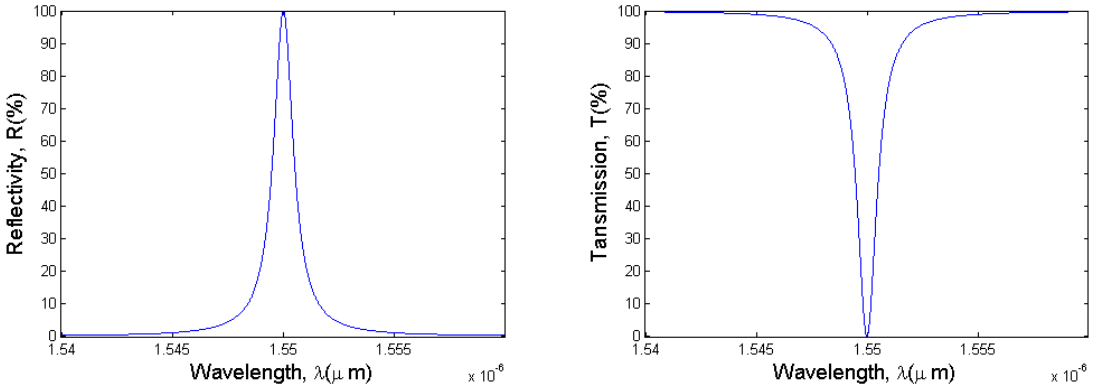

Figure 3.9: Ideal and theoretical reflectivity and transmission of an FBG with peak reflectivity @ 1.55 μm.

3.6 Dispersion

Dispersion is the broadening of a pulse. Broadening means that the pulse drops in power and broadens in time. Several sources of dispersion are known[1, p.355], and on of these is the material dispersion. For single mode fibers material dispersion arises from the wavelength dependence of the refractive index, $n(\lambda)$. This will make the frequency components of a pulse to travel at different speeds. The key value, given in specification sheets of optical fibers, is the material dispersion coefficient D_λ. By having the length of the fiber, L, and the spectral linewidth of the pulse, σ_λ, the broadening of the pulse can be found to be[1, p. 353]

$$\sigma_\tau = |D_\lambda| \, \sigma_\lambda L \tag{3.9}$$

where σ_τ is the response time of the fiber.

3.7 Losses

Intrinsic losses in silica fiber optic cables comes mainly from three sources[10]; UV absorption, infrared absorption, Rayleigh scattering gives rise to the attenuation per fiber length α. This attentuation varies for different wavelengths mainly because Rayleigh scattering is dependent on wavelength and goes as $\propto \frac{1}{\lambda^4}$. Wavelengths and materials also plays a key role as is shown in **Table 3.1**. The most common wavelength used today is 1.55 μm due to its low loss in silica fibers.

Cable	Type	λ(nm)	Attenuation
Thorlabs 1550BHP[11]	Silica	1460 - 1620	0.5 dB/km @ 1550 nm
Thorlabs SM1500G80[12]	Silica	1550 - 1700	$\leq$ 2 dB/km @ 1550 nm
Thorlabs SM400[13]	Silica	405 - 532	$\leq$ 30 dB/km @ 532 nm
Thorlabs 1060XP[14]	Silica	980 - 1600	$\leq$ 1.5 dB/km @ 1060 nm
Newport F-SM10[15]	PHC, Silica	above 400	$\leq$ 2 dB/km @ 1550 nm
PO MMPOF250[16]	POF, PMMA	N/A	$\leq$ 0.35 dB/m

Table 3.1: Loss for different fiber types and wavelengths.

Losses also occur when building an optical system. Splicing of fibers, the use of connectors and equipment loss all contribute to attenuation of the signal in a fiber. E.g. for splicing the attentuation can vary with technique; if done correctly, fusion splicing of single mode fibers can get as low as 0.02dB per splice[17, p. 4].

Chapter 4

Underwater surveillance and hydrophones

The following chapter will give an introduction to underwater surveillance and give an explanation of the working principles of fiber optic hydrophones.

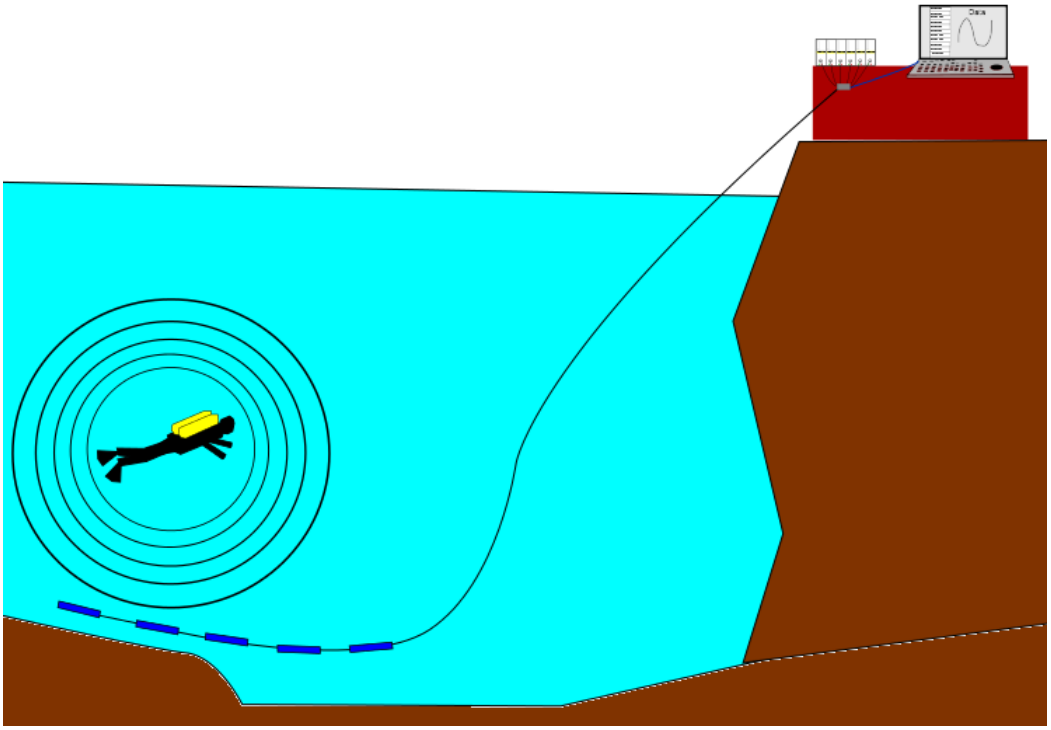

Figure 4.1: Diver detection by the use of a passive array of hydrophones.

4.1 Underwater surveillance and acoustics

There are two main concepts on detection of an acoustic signal underwater; active and passive. A SONAR is an example of active detection where an acoustic signal is sent out from a source in one or several directions. The signal gets reflected of an object and is then received by the source. The time it takes between the signal is sent and received is calculated, revealing the position of the object, much like a RADAR. This allows for detection of objects which does not have an acoustic signal. For passive detection, the principle is much like a microphone where no signal is sent out and the system only listens to acoustic signals. These systems have the benefit of not revealing that they are sensing, but they are dependent on a strong acoustic signal from the source. The signal they can detect are limited by the sensitivity of the system and the noise in the ocean. An example of a passive system is the hydrophone which can be described as an underwater microphone detecting changes in pressure. An example of the concept of passive detection is shown in **Figure 4.1**.

In underwater acoustic sensing it is differed between the *wet end* and *dry end*. These terms are quite self explanatory where the dry end is the part of the hydrophone(or hydrophone system) above the sea level and the wet end is the part that is below the sea level.

Common setups for hydrophone systems are the towed array, illustrated in **Figure 4.2**, and the acoustic tripwire, illustrated in **Figure 4.3**. A towed array works as an acoustic antenna that is dynamic in position. These arrays are usually being towed behind a vessel. The acoustic tripwire has a static position and has the working principle of a tripwire; an object "trips" on the sensor array when its acoustic signal is detected by the array.

The transmission loss of sound in water arises from the spreading of the acoustic wave when it propagates away from the source and the absorption of water. For a source with an isotropically spreaded acoustic signal the intensity becomes $I \propto \frac{p}{r^2}$, where p is the pressure and r is the distance from the source. Calculations of absorption have to be done by using algorithms which are dependent on frequency, temperature, depth/pressure, salinity and pH value. E.g. a 1 kHz acoustic signal propagating at 500 meters depth in a water with a temperature of 4 degrees, salinity of 35 ppt and a pH value of 8 can be found to be 0.064 dB/km by using the Ainslie and Mccolm formula[22]. The absorption is minimal at low frequencies

and the major contribution to transmission loss at low frequencies is the spreading of the acoustic wave.

In water the formula for the acoustic velocity becomes more complicated than described in Section 2.2. The parameters controlling the velocity of sound in water is the salinity, temperature and pressure. There are several formulas existing for determining the speed of sound, such as Del Grosso[23] and UNESCO[24].

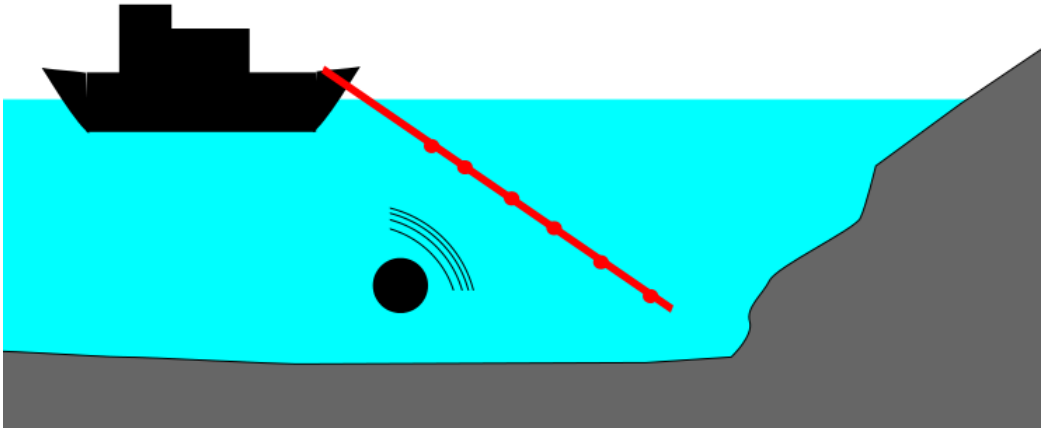

Figure 4.2: Towed array. The vessel drags an array(red) which can detect objects that produce acoustic signals.

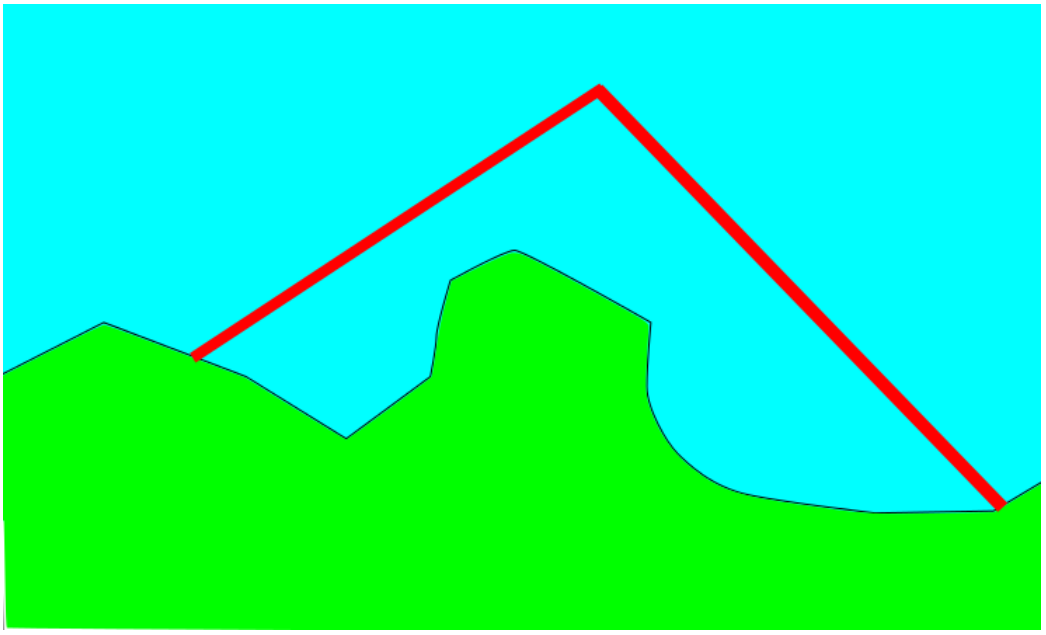

Figure 4.3: Acoustic tripwire. The tripwire(red) is seen from a birds view. It works by being lowered into the water(blue) and interrogated from land(green).

4.2 The piezoelectric hydrophone

The piezoelectric hydrophone has been the most common approach to detect sound waves in water. A conventional piezoelectric hydrophone consists of a piezoelectric material responding to changes in the acoustic pressure by creating an alternating voltage that is proportional to the acoustic pressure. The piezoelectric hydrophone has proven to be a good sensor of acoustic pressure, however, it has some disadvantages as listed in the introduction of this thesis. By using electrical cables and instrumentation the system can become unreliable due to corrosion and in some cases also electrical leakage. Also, if a sensor is situated in the water on a permanent basis the sensor can degrade because of fatigue in materials. Common sensitivities lies in the range of -210 to -180 dB re 1 V/μPa[25, p. 141].

4.3 The fiber optic hydrophone sensor head

An area which has been researched since the 1970s[26] is the use of a fiber optic cable for acoustic sensing. One of the most crucial components of a fiber optic sensing system is the sensor head. The sensor head works as a transducer converting the acoustic pressure to a response in the optical fiber, and can also detect changes in temperature. When designing the sensor head, special care must be taken because the sensor head is often what limits the final sensitivity of the system. Factors as operational environments must also be taken into account. Three sensing techniques exists for fiber optic hydrophones; change in intensity, change in phase and change in reflected wavelength.

4.3.1 Intensity based sensors

For intensity based sensors the acoustic wave creates changes in the amplitude of an optical wave by creating losses in the sensor head. These losses can be created by e.g. an acoustic wave inducing abrupt bends(microbends)[27] in the fiber or having two fiber ends close to each other where their alignment is a result of the acoustic wave[28, p. 224]. These structures can be easy to realize and usually has low cost because of their simple principle of operation and signal processing.

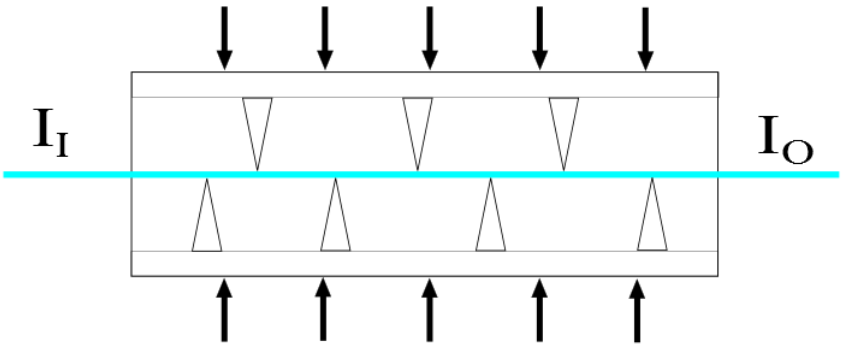

Figure 4.4: Working principle of the microbend sensorhead. An optical wave with intensity I_I experiences a loss in the sensorhead which gives the output intensity as I_0.

4.3.2 Phase and wavelength shifting

In phase shifting hydrophones the acoustic wave creates a phase shift $\mathrm{d}\varphi$ of an optical wave propagating in the fiber. The phase of a wave in a fiber is given by [2, p. 233]

$$\varphi = \beta L \approx n k_0 L \tag{4.1}$$

where n is the refractive index of the fiber core, k_0 is the optical wavenumber in free space and L is the physical length of the fiber. Differentiating equation (4.1) gives:

$$\frac{\mathrm{d}\varphi}{\varphi} = \frac{\mathrm{d}n_0}{n_0} + \frac{\mathrm{d}k}{k} + \frac{\mathrm{d}L}{L} \tag{4.2}$$

The dominant factor for relative phase changes when inducing strain in a fiber is the relative length change $\mathrm{d}L/L$[2, p. 265], which is the same as the expression for the longitudinal strain ε. Because of the photoelastic effect[2, p. 170] of materials the relative phase change cannot be written directly as $\frac{\mathrm{d}\varphi}{\varphi} = \varepsilon$, but becomes[29]

$$\frac{\mathrm{d}\varphi}{\varphi} = \xi\varepsilon \tag{4.3}$$

where ξ is the strain optic correction factor for an isotropic solid, given by

$$\xi = 1 - \frac{n^2}{2}\left[(1-\nu)p_{12} - \nu p_{11}\right] \tag{4.4}$$

where ν is the Poissons' ratio and p_{ij} are the strain optic tensor elements describing the mechanical response of the fiber.

Wavelength changing sensors uses FBGs to give a response to pressure. An acoustic wave will alter the length of the grating which creates a change in the reflected wavelength.

For fiber bragg grating sensors the relative bragg wavelength shift is given by[30]

$$\frac{\Delta\lambda_B}{\lambda_B} = \xi\varepsilon \tag{4.5}$$

which is exactly the same on the right side of the equal sign as equation (4.3).

4.4 Sensitivity

In acoustics, the pressure of a wave is often written in decibel(dB) instead of Pascal(Pa). A decibel is not really a unit but a ratio related to a given value. In air, the decibel is related to the lowest detectable pressure a human ear can detect, which is 20 μPa at 1m. For water this is related to 1 μPa at 1m. As an example, a sound pressure of 1 μPa corresponds to 0 dB re μPa in the water.

The sensitivity, which is also know as the normalized acoustic responsivity, is given by

$$S = \frac{\Delta\varphi}{\varphi\Delta p}. \tag{4.6}$$

To give an understanding of how the sensitivity impacts a hydrophone system it is essential to calculate what the lowest detectable phase change is. This corresponds to the sensitivity of the piezoelectric hydrophone where the hydrophone is limited by the lowest detectable voltage change. It is desired that acoustic signals with low pressures results in large enough changes in the phase that is to be detected. A lower sensitivity means a lower phase change by the incoming pressure. Objects

that are far away drops in acoustic amplitude, as explained in Section 4.1, and it is desired that one can measure signals down to the noise level of the ocean.

When designing a hydrophone system the final sensitivity of the system is limited by the noise. Noise can come from many sources; for a piezoelectric based hydrophone device the noise can have origins in both the acoustic incoming wave, and the electric noise in the system. The acoustic noise arises from the ambient noise in the ocean. Not much can be done to reduce the ambient noise than configuring the frequency response and the directivity of the sensor[25, p. 149]. The ambient noise can be found from the sea states shown in **Table 4.1**.

Sea state	Wind speed(knts)	Noise level(dB)
0	0	44.5
1	1-2	50
2	4-6	55
3	7-10	61.5
4	11-16	64.5
5	17-21	66.5
6	22-27	68.5-70

Table 4.1: Sea states and their corresponding noise levels[31].

4.5 Coating

A bare fiber itself does not respond to acoustic waves well. One approach to solve this has been to use polymer coatings to increase the acoustic sensitivity. Coatings are usually on the fiber in the form of a buffer or a jacket as explained in Section 3.1, and seen in **Figure 4.5**. A standard coating of a fiber is usually applied to make the fiber more robust and to shield it against damages and the environment, but special coatings of different materials and thicknesses can be applied to increase the acoustic sensitivity. The fiber can then be viewed upon as a composite made up by the fiber and the coating[32].

Coatings can degrade as a result of maritime conditions reducing the mechanical properties.[33]

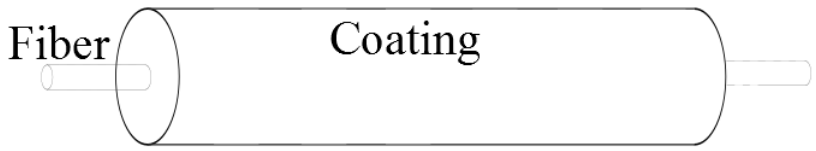

Figure 4.5: Single coating applied to fiber

4.6 Mandrel

Another approach for increasing the sensitivity have been the use of mandrels. The mandrel can be both hollow and filled. A mandrel induces strain in the fiber from an acoustic signal. An illustration of a fiber wound around a mandrel is shown in **Figure 4.6**.

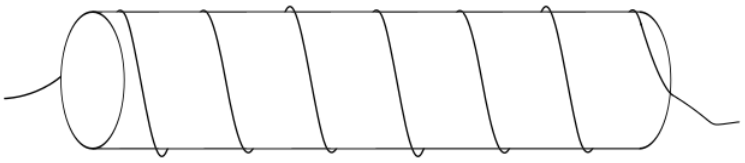

Figure 4.6: Fiber wrapped around mandrel.

When using a mandrel the radial strain can be expressed as. [2, p. 267]

$$\frac{\mathrm{d}r}{r} = \varepsilon_r = \frac{-p}{3K}. \tag{4.7}$$

In equation (4.7), p is the pressure, ε_r is the radial strain in the mandrel, r is the radius of the mandrel and K is the bulk modulus. The radial strain in the mandrel affects the longitudinal strain in the optical fiber by inserting equation (4.7) into equation (4.3) creating the relation

$$\frac{\mathrm{d}\phi}{\phi \mathrm{d}p} = \frac{-\xi}{3K}. \tag{4.8}$$

As a further expansion on the mandrel concept, hollow mandrels have been used. Their sensitivity can be expressed[34]

$$\frac{\mathrm{d}\phi}{\phi \mathrm{d}p} = \frac{-\xi r}{Et}(1 - \frac{\nu}{2}) \tag{4.9}$$

where r is the radius of the mandrel and t is the thickness. Equation (4.9) is usually only valid for $r/t \leq 10$[35].

4.7 Direction, angle and distance determination

For arrays, the spacing d between the sensor heads must satisfy the Nyquist condition for discretization of spatial functions[36, p. 263], such that $d \leq \frac{\Lambda}{2}$. Fulfilling this condition will reduce the side lobes of the directivity function $D(\theta)$, given by[36, p. 262]

$$D(\theta) = \frac{\sin\left(\pi \frac{d}{\Lambda} N \sin(\theta)\right)}{N \sin\left(\pi \frac{d}{\Lambda} \sin(\theta)\right)} \tag{4.10}$$

where N is the number of elements in the array and θ is the angle of an acoustic source with respect to the array. An object in a direction perpendicular to the array will be at an angle $\theta = 0^0$, which also is the angle where the maximum power of the acoustic wave is received. The reduction of side lobes gives a better directivity of the array. Increasing the distance between the sensors will create an altered directivity pattern which will give angles where no signal is detected at all and angles where the signal is at its maximum.

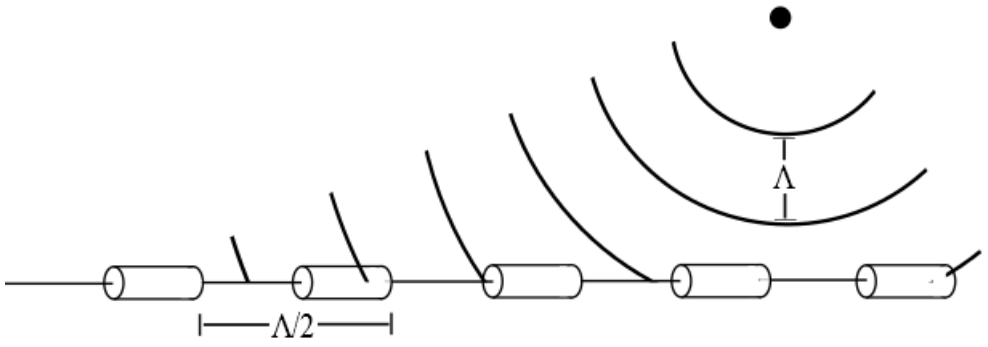

Figure 4.7: Incoming acoustic wave from a point source on a hydrophone array. The hydrophone sensor heads experiences a change in surrounding pressure at different times dependent on the position of the source.

A general formula for the distance between the sensors, d, is seen in equation (4.11). The equation for $\frac{\Lambda}{2}$ arises from the relation that $\Lambda = \frac{v_{\min}}{f_{\text{high}}}$, where $v_{\min}$ is the lowest speed of sound in water, explained in section 4.1, in which the array is operating.

$$d \leq \frac{\Lambda}{2} = \frac{1}{2}\frac{v_{\min}}{f_{\text{high}}} \tag{4.11}$$

If the Nyquist criteria is to be fulfilled the minimum amount of sensor heads for the array has to be

$$\#\text{sensors}_{\min} = \left\lceil \frac{l_{\text{a}}}{d} \right\rceil \tag{4.12}$$

where l_a is the active area of the array. Equations (4.11) and (4.12) clearly shows that higher frequency measurements gives a shorter distance between sensors which leads to a larger amount of sensors needed on the active area of the array.

Chapter 5

Hydrophone systems

When designing a hydrophone system several criterias has to be determined. One has to choose the operating acoustic frequencies, sensitivity, multiplexing scheme, cost, length, depth, weight etc. of the system. This chapter will introduce basic hydrophone systems and present calculations of sensor heads. All the values given in this chapter are theoretical and may differ from measured values.

5.1 Sensor heads

It is evident that the design of the sensor head plays a key role for the final system design. The basics is that the sensing head should to be able to create change in light that is measurable, for the least amount of strain. For bare fiber calculation the cladding and the core are assumed to have the same material properties and can then be viewed upon as a single medium.

To find the sensitivity of a bare fiber, there is need to start out with combining equations (4.3) and (4.4) to express the full equation for the relative phase change.

$$\frac{\mathrm{d}\varphi}{\varphi} = (1 - \frac{n^2}{2}\left[(1-\nu)p_{12} - \nu p_{11}\right])\varepsilon. \tag{5.1}$$

The strain now has to be related to the pressure of the surrounding wave to find how the strain is influencing the relative change in phase. In equation (2.24) the Young's modulus was defined. This equation can be rewritten as $\varepsilon = \frac{\sigma}{E}$, which is

also known as Hooke's law. For a cube the generalized Hooke's law can be written as [37]

$$\varepsilon_x = \frac{\sigma_x}{E} - \nu\frac{\sigma_y}{E} - \nu\frac{\sigma_z}{E} \tag{5.2a}$$

$$\varepsilon_y = -\nu\frac{\sigma_x}{E} + \frac{\sigma_y}{E} - \nu\frac{\sigma_z}{E} \tag{5.2b}$$

$$\varepsilon_z = -\nu\frac{\sigma_x}{E} - \nu\frac{\sigma_y}{E} + \frac{\sigma_z}{E}. \tag{5.2c}$$

A fiber is cylindrical such that the stress can only be longitudinal, $\sigma_l = \sigma_x$ or radial, giving $\sigma_r = \sigma_y = \sigma_z$. As for stress there is only longitudinal, $\varepsilon_l = \varepsilon_x$ and radial strain, $\varepsilon_r = \varepsilon_y = \varepsilon_y$. The longitudinal strain can then be written as

$$\varepsilon_l = \frac{\sigma_l}{E} - 2\nu\frac{\sigma_r}{E} \tag{5.3}$$

For a small object relative to the wavelength of an acoustic wave the experienced stress is isotropic. This means that there is hydrostatic boundary conditions and the strain is the pressure of the acoustic wave ($\sigma = p$). Under these condititions the longitudinal and axial strains are equal, $\varepsilon_l = \varepsilon_r = \varepsilon$, giving $\varepsilon = (1 - 2\nu)p/E$. The expression for the sensitivity under hydrostatic boundary conditions becomes

$$\frac{\mathrm{d}\varphi}{\varphi p} = \xi\frac{(1 - 2\nu)}{E} \tag{5.4}$$

For fused silica, material values are found to be[38]$p_{11} = 0.12$, $p_{12} = 0.27$, $n = 1.45$ and [39]$\nu = 0.17$, $E = 73.1$GPa, $K = 36.7$GPa. Inserting the values into equation (5.1) gives

$$\frac{\mathrm{d}\varphi}{\varphi} \approx 0.78\varepsilon. \tag{5.5}$$

This means that the photoelastic effect reduces the strain response by around 22% for the given values. Inserting the rest of the parameters for silica into equation (5.4) the sensitivity of a bare fiber is found to be -343 dB re $\mu\mathrm{Pa}^{-1}$.

Other materials can also be used as optical fibers as explained in Section 3.3 on page 22. For instance, polymers are often less stiff than silica, with respect to the Young's modulus and are therefore promising for increasing the sensitivity. Calculations on strain and temperature sensitivity have been performed earlier on polymethyl methacrylate(PMMA) by Silva-Lopez et.al.[40]. Silva-Lopez et.al. gives the Young's modulus of PMMA as $E \approx 2.8$ GPa and refractive index at 800 nm as $n \approx 1.49$. Values for the strain optic tensor are found to be $p_{11} = 0.3$, $p_{12} = 0.297$[41] with the Poisson's ratio $\nu = 0.35$[42]. Calculations give $\xi \approx 0.9$ which is about 16% better than for silica. The sensitivity is found to be -320 dB re μPa^{-1} for the given values, which is a gain of 23 dB with respect to the silica fiber.

For PHCs, also described in Section 3.3 on page 22, the calculations become more complicated[43] given their often anisotropic geometrically structured cladding. Measurements of the material parameters, such as the strain optic tensor elements, will have to done before calculation of sensitivities on these fiber types can be done.

One approach for increasing the sensitivity is to wound the fiber onto a mandrel, as explained in Section 4.6 on page 36. One interesting fact is that the sensitivity is inverse proportional to the bulk modulus of the mandrel, as seen in equation (4.7). In **Table 5.1** sensitivities for mandrels of different materials with wound silica fiber are calculated using equation (4.7). The calculations in **Table 5.1** shows that polymers can achieve a theoretical gain of $\approx$ 20 - 30 dB on the silica fiber, whereas metal gives a negative gain $>$ 6 dB.

Material	E(GPa)	ν	K(GPa)	S (dB re μPa^{-1})
Nylon-6[44]	2.1	0.39	3.18	-321
PMMA[42]	2.8	0.35	3.11	-321
Polycarbonate[45]	2.3	0.31	2.01	-318
Polyethylene[46]	0.7	0.42	1.46	-315
Aluminium[47]			70	-349
Steel[47]			160	-355

Table 5.1: Theoretical mandrel sensitivities for different materials with values given in the table. The top four elements are polymers and the bottom two are metals. The strain optic correction factor for silica fiber was calculated with [38]$p_{11} = 0.12$, $p_{12} = 0.27$, $n = 1.45$ and [39]$\nu = 0.17$. The Bulk modulus was calculated from the values of the Young's modulus and Poisson's ratio using equation (2.26) when it was not given. MATLAB script is given in appendix A.1.

It is desired to keep the mandrel radius as low as possible to e.g. reduce weight, materials cost and keeping the structure smaller than the acoustic wavelengths that are to be measured. Losses in the sensor heads can occur with small mandrel radii because the fiber is wound onto the mandrel. Silica fibers are based on the principle of total internal reflection, which were explained in Section 3.1, and if bent, they can couple light into the cladding. Losses can also arise from that the bending causes mechanical deformation in the fiber, which is known as microbending. For very low radii the fiber can also break.

Hollow mandrels have been used to further increase the sensitivity of mandrels. **Table 5.2** shows theoretically calculated values of sensitivity using equation (4.9) with $r/t = 20$. The use of hollow mandrels clearly increases the sensitivity for all the materials with a gain of 40 dB for polyethylene.

Material	E(GPa)	ν	S(dB re μPa^{-1})
Nylon-6	2.1	0.39	-284
PMMA	2.8	0.35	-287
Polycarbonate	2.3	0.31	-285
Polyethylene	0.7	0.42	-275
Aluminium	68	0.33	-314
Steel	210	0.29	-323

Table 5.2: Theoretical values for the sensitivity of hollow mandrels. The materials and silica values are the same as in **Table 5.1**. Equation (4.9) is used with a ratio of $r/t = 20$. MATLAB script is given in appendix A.2.

Coating of the fiber was introduced in Section 4.5. This approach encapsulates the fiber for the purpose of increasing the sensitivity, but can be hard to calculate. Modal analysis and software can be used for these calculations. The given techniques can also be combined. Junghare et. al.[48] combined a hollow mandrel with a coating by using ANSYS to apply modal analysis in the calculation of the sensitivity.

The sensitivity for an FBG will be the same as the calculations done in this section because the formulas for wavelength change in equation (4.5), and phase change in equation (4.3), are the same.

5.2 Single hydrophone

A hydrophone system with one sensor head is ideal to start out with to show how the sensitivity affects a system. For the following calculation a Mach-Zender interferometer setup, shown in **Figure 3.4**, and a phase shifting sensor head is used. The length of the fiber needed to detect a low acoustic signal can be determined from a theoretical value of the minimum detectable phase change $\mathrm{d}\varphi = 1$ μrad in a detector. From equation (4.3) an expression for the length of the fiber needed in the sensor head can be found as

$$L = \frac{\mathrm{d}\varphi\lambda}{2\pi n S \mathrm{d}p} \tag{5.6}$$

By using sensitivity $S = -315$ dB re $\mu\mathrm{Pa}^{-1}$ for a fiber wound on a polyethylene mandrel, wavelength $\lambda = 1.55\mu$m, acoustic pressure amplitude of $\mathrm{d}p = 100\mu$Pa and a refractive index $n = 1.45$, the length is found to be $L = 9.6m$. This then corresponds to the amount of fiber needed in the sensing arm to create a high enough phase change to be detected.

When using a interferometer, the signal has to be demodulated such that the acoustic signal can be recreated by the signal processing equipment. For demodulation the output signal of an interferometer was given in equation (2.12) as $I = 2I_0\left[1 + \cos\left(\varphi\right)\right]$. For simplicity reasons $2I_0 = P$ is chosen as the amplitude and from equation (2.13) the photocurrent after differentiation becomes

$$i_p = \Re P \cos(\mathrm{d}\varphi) \tag{5.7}$$

Where $\Delta\varphi$ is, as explained earlier, the phase difference between the wave in the reference and sensing arms. By another simplification, $\mathrm{d}\varphi = \varphi_r - \varphi_s \sin(\Omega t)$ this can be rewritten as

$$i_p = \Re P \cos(\varphi_r - \varphi_s \sin(\Omega t)) \tag{5.8}$$

where φ_r is the phase in the reference arm, , φ_s is the phase of the sensing arm and $\sin(\Omega t)$ is taken from equation (2.16) such that it is directly related to the pressure of the acoustic wave. This is in general not true, however the phase in

the sensing arm will be proportional to that signal. A problem arises when high acoustic amplitudes are present. High amplitudes create a high difference in path length which will create errors in the interferometric setup. This is given as an example in **Figure 5.1**.

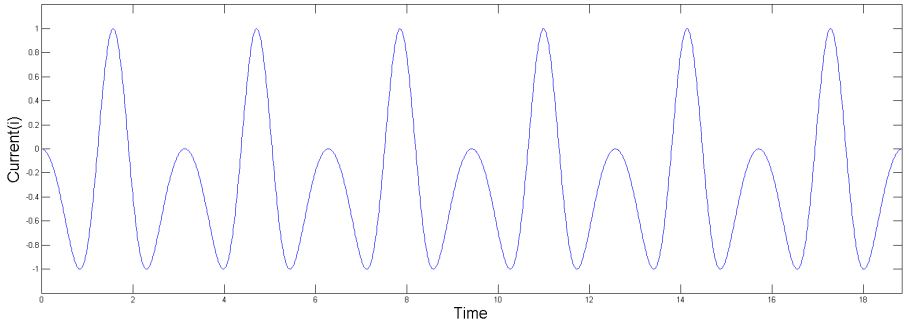

Figure 5.1: Distorted signal output after photodetector due to high amplitude of sensed acoustic signal.

This will limit the dynamic range, described in Section 4.4, because the higher amplitudes creates distortions in the interferometric signal. One approach to this is to use homdyning[2, p. 239]. Using active homodyne this can be fixed by creating a feedback loop from the output connected to a piezoelectric element. The piezoelectric element in the reference arm creates strain in the reference arm fiber, which is seen in **Figure 5.2**. This will alter the phase and minimize the path difference to keep the output out of saturation. This will be directly related to φ_r in equation (5.8). Passive homodyne, such as phase generated carrier(PGC)[49] can also be used to remove this problem.

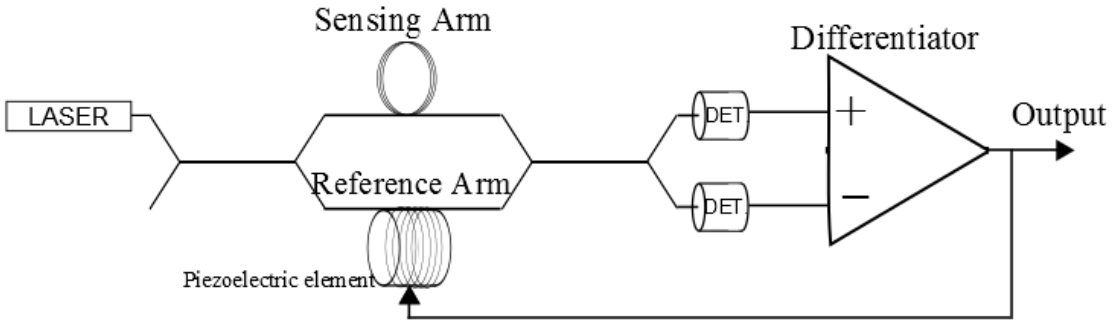

Figure 5.2: Setup of active homodyne in an interferometer using a piezoelectric element in the reference arm[2, p. 241]. The piezoelectric element expands and retracts as a result of the output signal, which causes a strain in the reference arm.

5.3 Arrays

The use of arrays were explained in Section 4.1. Larger areas can be covered by using arrays, and the signals from several hydrophones can provide a more directive array.

5.4 Superluminescent source and FBGs

In Section 2.1.1 lasers were discussed and it was focused on that they had the benefit of achieving a narrow spectral width. However, by using a superluminescent LED source, which has a broad spectral width $\Delta\lambda$, the FBG based sensor can be put to use. The working principle is that a superluminescent source sends a broad wavelength range into an array with FBGs, as shown in **Figure 5.3**. Each FBG is manufactured to reflect at a different peak wavelength, λ_b. A change in λ_b occurs when pressure is incident on the grating. The reflected wavelengths are then sent into a WDM demultiplexer which separates the wavelengths onto different fibers. Each signal can then be read out by a spectrum analyser.

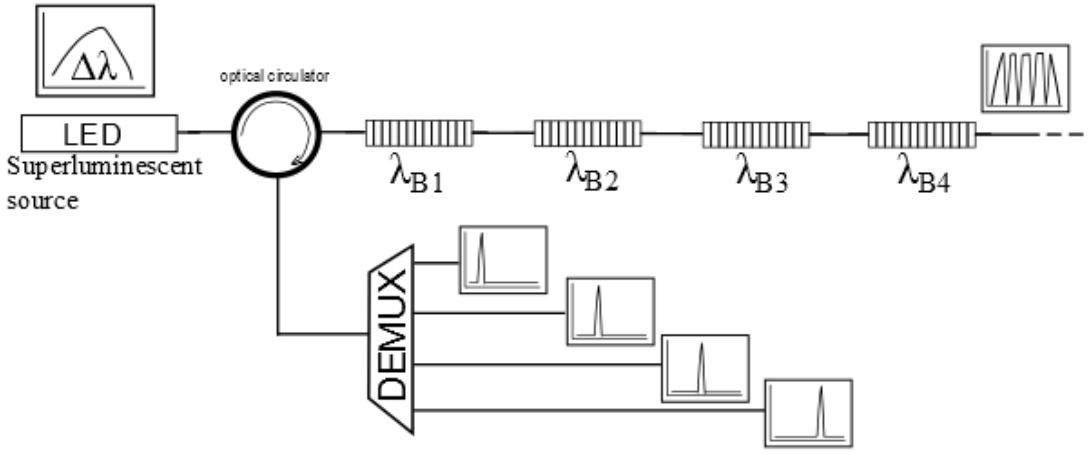

Figure 5.3: A system operating with FBG sensors and a superluminescent source. The superluminescent source has a broad spectral width and the spectral components are reflected by FBGs with different peak wavelengths. The reflected wavelengths are sent into a demultiplexer which splits the wave. The reflected wavelength can be found a spectrum analyzer. A change in pressure at a FBG causes the peak reflected wavelength, λ_B to change.

Superluminescent sources can have spectral widths $\Delta 80 - 100nm$ which can give a high amount of sensors. One drawback is that they don't have the same intensity for all wavelengths.

5.4.1 TDM based array

TDM based arrays have been proposed in a variety of architectures[3, p. 380]. One proposed architecture is the use of a circulator in combination with FBGs, as shown in **Figure 5.4**. The system uses one wavelength and is pulsed using a modulator or a pulsed laser. Each FBG has to have low reflectivity and be configured to have a peak reflection wavelength λ_b corresponding to the operating wavelength of the system. For each pulse that is sent into the system, several pulses with lower power are generated. The acoustic pressure on each sensor creates a difference in the interval, τ, between each reflected pulse. This system is limited to that only one operating wavelength is used such that the power drops for each FBG reflection, minimizing the number of sensors that can be used for the system.

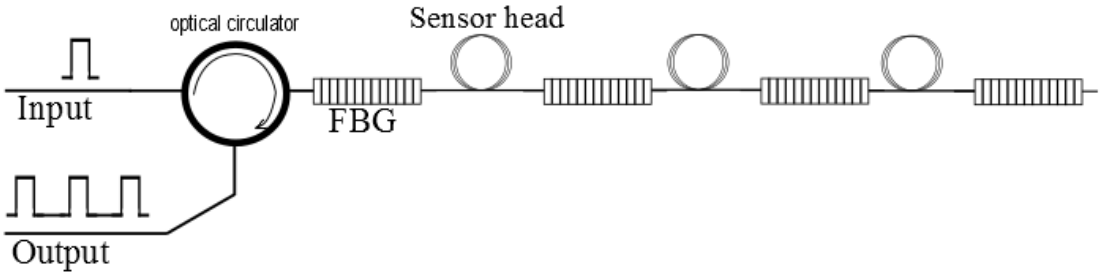

Figure 5.4: TDM architecture for hydrophone system[3, p. 381]. An array is pulsed and reflections are created by low reflecting FBGs. The interval between each reflected pulse corresponds to the acoustic pressure present on the sensor head. The circulator prevents pulses from going back into the lasers.

5.4.2 WDM based array

This architecture is based on that each wavelength is assigned to a sensor head in the array. N wavelengths are sent into a WDM multiplexer, seen in **Figure 5.6**, which combines the wavelengths onto a single fiber. The sensor head, shown in **Figure 5.5**, has an FBG on both sides, and by pulsing, the interval between the reflections of the FBGs is become affected the strain in the sensor, like the TDM system.

The benefit of this is that the FBGs can

This system is limited by that the operating wavelengths are not infinite. The FBGs quality, in terms of bandwidth and reflectivity, controls the spacing between the wavelengths that can be used.

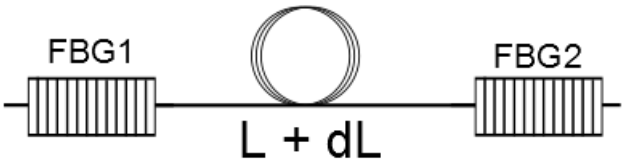

Figure 5.5: Sensor head of WDM system. The sensor head consists of an FBG on both sides of a sensing coil. When and acoustic pressure is present the coil will change in length, creating changes in interval between the reflections.

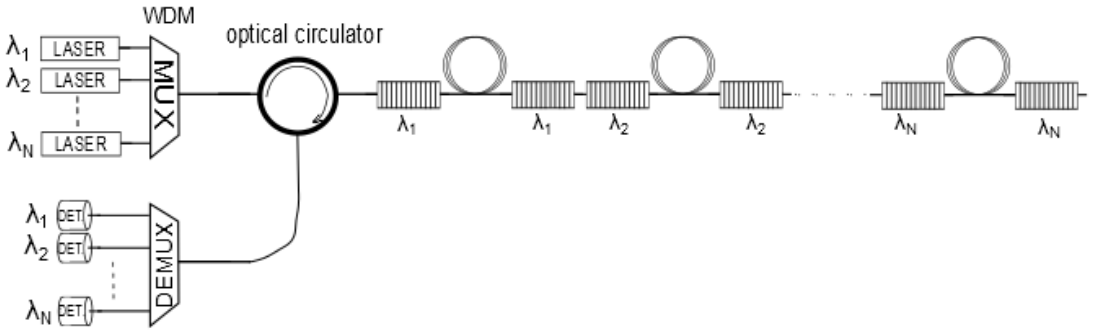

Figure 5.6: WDM hydrophone array with N channels[3, p.383]. Each channel corresponds to a wavelength which is assigned

5.4.3 Hybrid multiplexing using WDM/TDM

Another way of making an array is to combine multiplexing techniques a hybrid multiplexing architecture based on the previously explained WDM and TDM architectures. The system is patented[4] and is seen in **Figure 5.7**.

The system is divided into subarrays where each subarray works as the WDM architecture explained earlier. Using subarrays incorporates the TDM architecture into the system giving the total number of sensors to be N x M. Each sensor head consist of two fiber bragg gratings and a sensing coil, which is the same as shown in **Figure 5.5**. This will minimize the reflection problem which the TDM scheme has where each FBG can create multiple reflections of pulses because of only one operating wavelength. If one chooses 64 sensors, the optimal thing would be to use 64 wavelengths, but this would make the array extremely expensive. A combination of 8(N) wavelengths with 8(M) subarray is a more realizable setup.

For this system, splicing losses will play a significant role. Each FBG is spliced onto the fiber, and each splice has a loss of around 0.02dB, if done correctly. This means that each sensor head, which consists 4 splices, will have have a loss of $0.02 \times 4 = 0.08$dB. The pulse travelling to the 64th sensor will experience a loss

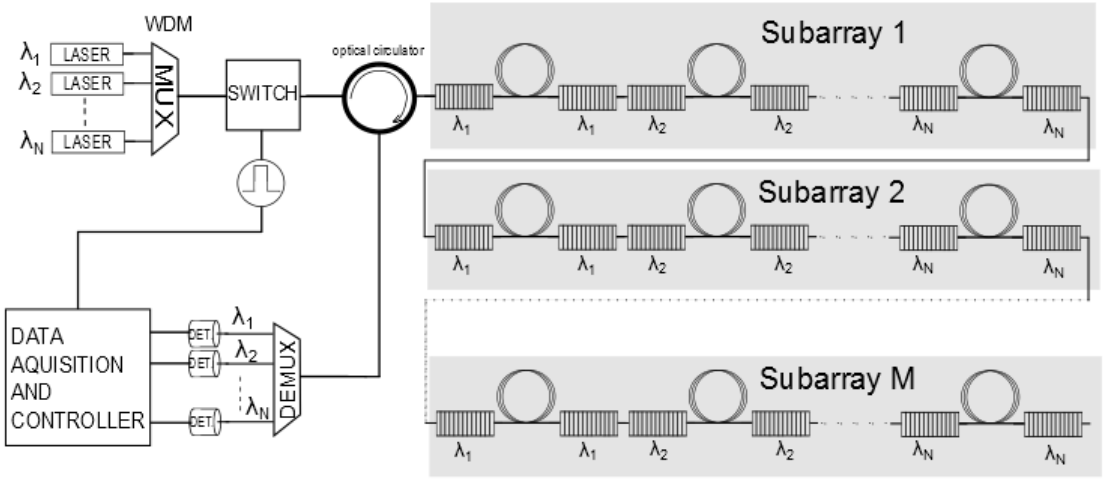

Figure 5.7: Hybrid WDM/TDM system[4]. The system has N wavelengths operating on M subarrays, creating the total amount of sensors to be N x M. Several wavelengths are multiplexed onto a fiber an pulsed by an external modulator or switch. Portions of pulses of the different wavelengths are reflected back by the FBGs, creating a pulse pair for each sensor head. The difference in time between each pulse pair corresponds to a.

at every splice twice, because it has to travel to the end of the fiber and back. The splice loss experienced by this pulse achieves a loss of $0.08 \times 64 \times 2 \approx 10.2$dB reducing it's power to around 10%. If splices are not done good enough losses can become even higher.

Given 8 operating wavelengths, means that 16 fiber bragg gratings(2 FBG pr sensor head) needs to reflect a portion of a wavelength back. This will also affect pulses travelling towards the end of the fiber. Losses also occur in multi-/demultiplexers, switches, circulators, splices and fibre loss. A solution to these losses is to branch out each subarray with a coupler. This will create a coupling loss, however this loss can be made lower than the loss that occurs in all the splices.

Another solution is to amplify the array. This can be done by having active fibers in portions of the system. A pumping wavelength amplifies the already present wavelengths propagating in the fiber without distorting them. The use of amplification also amplifies the noise.

5.4.4 Distributed feedback fiber laser (DFB-FL)

The DFB-FL consists of a sensorhead containing two FBGs which are structured to reflect at the same peak wavelength, λ_B. The two FBGs are written into an

active portion of a fiber with a distance of $\lambda_B/4$ between them. When pumped at wavelength corresponding to the doped material in the active fiber, the FBGs will act as a laser cavity creating a laser wavelength with center frequency of λ_B. External pressure will cause a shift in the bragg wavelength which results in a change in laser frequency. The sensor head can be seen in **Figure 5.8** and the total system in **Figure 5.9**.

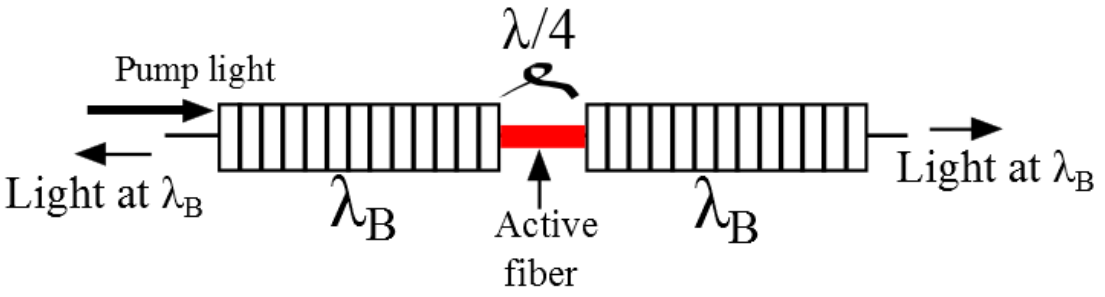

Figure 5.8: Sensor head for the DFB-FL[**?**]. An active fiber is pumped and the two FBGs acts as a laser cavity creating a

The benefit of this is that the FBGs can create wavelengths that can propagate independent of each other and be demultiplexed into fibers. Only the pumping wavelength is needed for operation

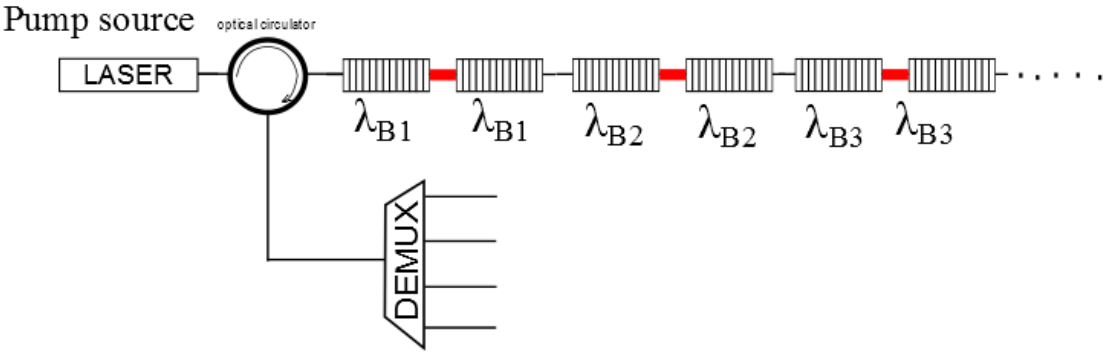

Figure 5.9: A DFB-FL array. A pumping source is incident on laser cavities created by the FBGs. The change in laser wavelength emitted from the FBG-pair corresponds to the change in acoustic pressure.

Chapter 6

Discussion

The following chapter will discuss the results and systems provided in the previous chapter to get a better understanding of how a hydrophone system can be designed. As stated in the introduction, fibre optic hydrophones cover several scientific field and prioritizing have been done for this thesis. It is important to understand that the values calculated in this thesis are theoretical and may differ from measured values.

6.1 Sensor heads

All calculations performed in the previous chapter have been temperature independent, since the focus of this thesis was to detect acoustic signals. The formulas used in the calculations of sensitivity can also be expanded to included the change in phase and wavelength as a function of changed temperature.

In all of the calculations for the sensor heads, a lower Young's modulus of the materials provided a higher sensitivity. The photoelastic effect also played a role in these calculations. It was shown that the PMMA based POF had a 16 % better strain optic correction factor, ξ, than the bare silica fiber. The combination of a higher ξ and a lower Young's modulus increased the sensitivity by 23 dB, which is a significant gain. POFs, however, have high attenuation which could be a big drawback for systems with many sensor heads.

Winding the fiber on a mandrel provided an increase in sensitivity, with respect to the silica fiber. The use of polyethylene showed that a theoretical gain on the silica

fiber to be 28 dB could be achieved. All the polymers showed an increase in the sensitivity and the metals showed a decrease. A decrease in sensitivity for metals, with respect to the silica fibers are directly related to their bulk modulus. The bulk modulus itself is related to the Young's modulus and Poisson's ratio, but the Young's modulus is clearly dominating for high values. Sensitivity calculations of the mandrel is independent of the radius, but it is known that a lower radius gives higher loss from bending in the fiber. When designing a mandrel based sensor head the fiber bend loss at different radii must therefore be taken into account.

Calculations for hollow mandrel were also produced. These calculations showed an even higher gain than for the solid mandrel based sensor heads. Again, the polyethylene provided the highest gain, now at 68 dB, but note again that this is a theoretical value. Using a hollow mandrel now provided an increase in sensitivity for the metals. It should be remembered that the equation used for calculation is only valid for thin cylinder walls, with respect to the radius, such that this criteria is obeyed.

In all the calculations the ultimate tensile strength has not been taken into account. Silica generally has a hight ultimate tensile strength, but when using mandrels, both hollow and filled, the ultimate tensile strength must be taken into account to see at what depths the sensor head can operate. This is especially important for hollow mandrels. The thickness of the cylinder walls were defined to be thin with respect to the radius and the absence of a core in the cylinder can make materials with low tensile strength break easily. A theoretical formula is even provided for this due to its importance. For high depths, a low sensitivity can actually be preferred because it is directly related to strain induced in the fiber(and mandrel). By lowering the sensitivity by using e.g. metals as mandrels, the strain transfer at high pressure can be lowered.

The use of a simulation software seems beneficial in designing a sensor head. A software can give a theoretical calculation of the e.g. frequency response and resonance frequencies. A frequency response can vary at different depths and simulations can therefore provide indications before this is measured. Software can also be used to choose coating materials and their dimensions, which were only introduced briefly in this thesis.

For directivity, the sensors discussed are omnidirectional given their cylinder shape which makes it hard to detect which direction the wave is coming from. The use

of a line array described in Section 4.7 can increase the directivity of the sensors and provide for detection of an angle and distance an object is present. To make single fiber optic hydropones with directivity further research is needed.

If one could use an optical fiber with better elasto optic coefficients ,in terms of strain transfer, a higher sensitivity can be achieved. Having a better strain optic correction factor in combination with a Young's modulus seems to be promising for increasing the sensitivity. An interesting approach would be to combine a hollow mandrel, with a POF and an acoustic pressure sensitive coating. For polymer optical fibers there are a variety of materials that can be used, but one most know the strain optic coefficients to determine the

Regarding the sensing technique, it would seem like intensity based sensors, explained in section 4.3.1, is better suited for single sensor heads. The stress applied to the sensor head attenuate the signals, which differs from the wavelength and phase shifting techniques that only changes the propagation constants.

6.2 Fiber type and material

SM fibers is the most used in fiber optic systems. This thesis have only mentioned how a MM fiber differ from the SM in terms of modes, and have not provided any examples on how MM fibers can be used for sensing. This may come from that the ; fiber have the benefit that only one mode propagates at a time which limits the dispersion.

PM fibers where mentioned in Section 3.3. The use of a PM fiber optic cable makes the wave maintain the polarization along the whole fiber length. The use of a PM fiber could prove beneficial because the bends, turns and external perturbations of the sensing arm in an interferometry system can alter the polarization, creating a faulty output as discussed in Section 2.1.3. It should be noted that a Faraday rotator, instead of a mirror, will have to be used such that the polarization is maintained if a PM fiber is used in a Michelson interferometer.

Most of the systems used and discussed operate at 1.55 μm. This wavelength is often chosen because it has a low attenuation. Another benefit is that WDM wavelengths are available in big wavelength band around 1.55 μm. ;any components are also designed specifically for operation around 1.55 μm because of the

wavelengths significance in communications systems. Other wavelengths can also be useful and if an operating wavelength of $\lambda = 1.55\mu$m/2 where used in a sensing system, then by equation (5.6) a reduction in the needed length of fiber a sensing arm will be reduced to L/2).

Silica fibers are the most used fibers. For photonics crystal fibers and plastic fibers the Young's modulus seems to be lower, but bend losses seems to be higher than in silica fibers. PHCs are usually made out of silica, but can be made out of other materials as well. The plastic fibers however are often softer because of their polymer materials.

Dispersion was explained for SM fibers in Section 3.6. This was not calculated for systems in this thesis, but must be taken into account when operating at long lengths of fiber. If fast pulses are used the dispersion of the fiber can broaden the pulse so much that crosstalk is achieved and faulty measurements are detected.

6.3 Applications

For towed arrays the total length fiber has to include the length from the ship to the active array. A long fibre is often needed from the ship can create noise that will easily be picked up by the array if close, however some vibrations can propagate from the boat and into the stretched fiber. This noise may be attenuated by packaging such that the vibrational noise from sources other than those to be measured is limited.

The losses in the different components such as the multi- and demultiplexer, circulator, sensor head, splicing losses etc. will contribute to the sensitivity of the final system which also is determined by the optical detectors.

6.4 Systems and multiplexing

The previous chapter introduced architectures base on TDM, WDM, WDM/TDM, superluminescent sources and DFB-FL and all of these schemes are proven to work. The system that should be selected is dependent on the purpose and specifications sensor count, cost of components, availability etc., have to be set.

The TDM scheme, in Section 5.4.1, showed that an FBG between each sensor head could create reflections for a pulse. Using only one wavelength means that all the FBGs must operate at the same wavelength wich can create multiple reflections between the FBGs. This effect will only get stronger with an increased amount of sensors, which in the worst case can create severe crosstalk that will make the system unusable. For low sensor numbers it can be a cheap and good solution because it only uses one laser, a circulater and a number of FBGs corresponding to

Using different wavelengths on a somewhat similar scheme was the basis for the WDM scheme, which were introduced in Section 5.4.2. Each sensor head had a FBG on both sides. Every sensor head were assigned to a wavelength that was determined the Bragg wavelength of its neighbouring FBGs. This removes the problem that the TDM architecture has with multiple reflections from each grating. This architecture can in principle be made for as many wavelengths that exist, only limited by how good the FBGs are in terms of bandwidth and reflectivity. However, this is not a very economic way to create a system of many sensors. WDM lasers can be prized at around 2500$ a piece which will make big sensor count systems extremely expensive. These systems are also limited by the amount of channels that can be demultiplexed, and high-channel count demultiplexers can be expensive.

The superluminescent FBG architecture in Section 5.4 provides for several wavelengths to be reflected by using only a source in combination with FBGs. The same is for the DFB-FL which creates several

Now that WDM has the ability to put several wavelengths inside a small band the capacity for the number of sensor heads can be increased. The ability to operate in a small band around 1.55 μm gives that each wavelength propagates with minimum attenuation in the fiber, since 1.55 has proven to be the wavelength with the lowest attenuation. WDM is the most popular multiplexing technique of communication system and components become more easily available, and will be even more with time. For high channel count WDM systems the problem is that components can get expensive, however the amount of use may have a mass effect lowering the prices of WDM components in the coming years.

6.5 FBGs

Many of the systems discussed have shown that they are dependent on an FBG to function. Section 3.5 discussed how the bandwidth and peak wavelength reflectivity could be customized by the grating length and strength. Small alterations in these values or faulty calculations can create catastrophic results if e.g. this happens in the first FBG of a single fiber. It is therefore crucial that the FBGs are constructed thoroughly as they are key components for several of the hydrophone system approaches. Apodization of the grating were also discussed to reduce the sidelobes causing reflections at other wavelengths.

For fused silica the splicing loss was given earlier to be 0.02 dB/km. It was shown that for a system with many FBGs that high losses could occur since each FBG needed a splice on each side. One way of overcoming this to have thee whole fiber photosensitive such that the FBGs can be written directly to the cable. This means that one must be extremely accurate if the fiber has to be wound on a mandrel later

Chapter 7

Conclusion

In this thesis, theory and explanations have been given to show how a fiber optic hydrophone can be used as an acoustic detector. The focus has been on giving solutions to the points given in the problem description.

Calculations have been made to show that the acoustic sensitivity of bare silica fiber is ≈ -343 dB re μPa^{-1}. This sensitivity can be improved with mandrels of different materials. By winding a fiber around a solid mandrel with a polymer material, the sensitivity is increased by 20 - 30 dB. The radius is arbitrary in terms of sensitivity, but a smaller radius gives a higher attenuation in the fiber because of bend losses.

For a hollow mandrel, the radius can not be chosen arbitrary, and the thickness of the cylinder wall must be kept at a ratio related to the radius. If this ratio is kept constant the sensitivity of the hollow mandrel will not be altered, but a smaller radius will again increase the bend loss. A small radius with this approach also decreases the strength against surrounding pressure.

Making antennas with a large number of hydrophones is theoretically possible with fiber optic systems using wavelength division multiplexing (WDM). These systems can either consist of a hybrid technique, which combines WDM with another multiplexing scheme, or by the use of distributed feedback lasers(DFB-FL). The DFB-FL scheme has been shown to have the benefit of only using one laser which can reduce the cost of a system.

The FBG has proven to be a key component independent on the system architecture that is used. FBGs can be manufactured with specific bandwidths and

tailored peak reflections. A major disadvantage of the FBG is that it is often spliced onto a fiber cable which creates a loss on each side of the grating. This reduces the power in the system for each grating used, which for a high sensor count, could use the need for amplification.

7.1 Future work

By providing the amounts of theory this thesis should be a small, but significant starting point for designing a fiber optic sensing system. Several things are thought to be done for future work.:

- It is recommended that the sensor head becomes a the starting point and that system is built around this.
- For the sensor heads measurements and simulations have to be done. One of the unanswered things of this thesis was the impact of a coating on the sensitivity. Simulating coatings and mandrel based sensor heads with modal analysis software could provide for a better understanding in the field of
- Another approach is to create a sensor head design that allows for detection of direction of a wave, meaning that the sensor head is directional.
- Signal processing
- Building a complete system

Bibliography

[1] B.E.A. Saleh and M.C. Teich. *Fundamentals of Photonics*. John Wiley & Sons, second edition, 2007. ISBN 978-0-471-35832-9.

[2] Eric Udd and William B. Spillman Jr. *Fiber Optic Sensors - An Introduction for Engineers and Scientists*. John Wiley & Sons, second edition, 2011. ISBN 978-0-470-12684-4.

[3] Shizhuo Yin, Paul B. Ruffin, and Francis T. S. Yu. *Fiber optic sensors*. CRCpress, Taylor & Francis Group, second edition, 2008. ISBN 978-1-4200-5365-4.

[4] Alan D. Kersey. ARRAY TOPOLOGIES FOR IMPLEMENTING SERIAL FIBER BRAGG GRATING INTERFEROMETER ARRAYS. U.S. Patent 005987197A, filed November 07, 1997, and issued November 16, 1999.

[5] John P. Dakin and Robert G. W. Brown. *Handbook of Optoelectronics*, volume II. Taylor and Francis Group, 2006. ISBN 9780750306461.

[6] Rüdiger Paschotta. Noise in laser technology. *Optik & Photonik*, 48(2):48–50, 2009.

[7] Paradigm optics. Polymer Optical Fiber and Monofilament. `http://www.paradigmoptics.com/pof/pof.html`, . [Webpage; accessed 28-MAY-2014].

[8] ITU. G.694.1: Spectral grids for WDM applications: DWDM frequency grid. `https://www.itu.int/rec/dologin_pub.asp?lang=e&id=T-REC-G.694.1-201202-I!!PDF-E&type=items`. [Online PDF; accessed 28-MAY-2014].

[9] Sunita Ugale and V. Mishra. Fiber bragg grating modeling, characterization and optimization with different index profiles. *International Journal of Engineering Science and Technology*, 2(9):4463–4468, 2010.

[10] John A. Buck. *Fundamentals of Optical Fibers*. John Wiley & Sons, second edition, 2004. ISBN 978-0471-221913.

[11] Thorlabs. 1550BHP Specificiations. `http://www.thorlabs.de/thorcat/12600/1550BHP-SpecSheet.pdf`, . [Online PDF; accessed 03-JUNE-2014].

[12] Thorlabs. SM1500G80 Specificiations. `http://www.thorlabs.de/thorcat/22100/SM1500G80-SpecSheet.pdf`, . [Online PDF; accessed 03-JUNE-2014].

[13] Thorlabs. SM400 Specificiations. `http://www.thorlabs.de/thorcat/24300/SM400-SpecSheet.pdf`, . [Online PDF; accessed 03-JUNE-2014].

[14] Thorlabs. 1060XP Specificiations. `http://www.thorlabs.de/thorcat/11300/1060XP-SpecSheet.pdf`, . [Online PDF; accessed 03-JUNE-2014].

[15] Newport. F-SM10 Specificiations. `http://assets.newport.com/webDocuments-EN/images/F-SM10_Datasheet.pdf`. [Online PDF; accessed 03-JUNE-2014].

[16] Paradigm optics. Polymer optical fiber and monofilament. `http://www.paradigmoptics.com/pof/pof.html`, . [Webpage; accessed 29-APR-2014].

[17] Fiberoptic.com. Fusion Splicing Today's Single mode Fibers. `http://www.fiberoptic.com/newsletter_images/specs/fusionsplicing.pdf`. [Online PDF; accessed 19-MAY-2014].

[18] Govind Agrawal. *Nonlinear Fiber Optics*. Academic Press - Elsevier, fifth edition, 2013. ISBN 978-0-12-397023-7.

[19] Govind P. Agrawal. *Applications of Nonlinear Fiber Optics*. Academic Press, second edition, 2008. ISBN 978-0-12-374302-2.

[20] RP Photonics. Effective Mode Area. `http://www.rp-photonics.com/effective_mode_area.html`, . [Webpage; accessed 21-APR-2014].

[21] RP Photonics. Nonlinear index. `http://www.rp-photonics.com/nonlinear_index.html`, . [Webpage; accessed 13-MAY-2014].

[22] Michael A. Ainslie and James G. McColm. A simplified formula for viscous and chemical absorption in sea water. *Journal of the Acoustical Society of America*, 103(3):1671–1672, 1998.

[23] V.A. Del Grosso. New equation for the speed of sound in natural waters (with comparisons to other equations). *Journal of Acoustics Society America*, 56 (4):1084 – 1091, 1974.

[24] C-T. Chen and F.J. Millero. Speed of sound in seawater at high pressure. *Journal of Acoustics Society America*, 62(5):1129 – 1155, 1977.

[25] Oscar Bryan Wilson. *Introduction to Theory and Design of Sonar Transducers*. Peninsula Publishing, 2011 edition, 1988. ISBN 978-0-932146-22-9.

[26] J. A. Bucaro, H. D. Dardy, and E. F. Carome. Optical fiber acoustic sensor. *Appl. Opt.*, 16(7):1761–1762, 1977.

[27] Fei Luo, Jingyuan Liu, Naibing Ma, and T.F. Morse. A fiber optic microbend sensor for distributed sensing application in the structural strain monitoring. *Sensors and Actuators A: Physical*, 75(1):41 – 44, 1999.

[28] Asit Baran Maity. *Optoelectronics and Optical Fiber Sensors*. PHI Learning Private Limited, 2013. ISBN 978-81-203-4781-6.

[29] C. D. Butter and G. B. Hocker. Fiber optics strain gauge. *Appl. Opt*, 17(18): 2867–2869, 1978.

[30] W. W. Morey, G. Meltz, and W. H. Glenn. Fiber optic bragg grating sensors. *Proc. SPIE*, 1169:98–107, 1990.

[31] D. de Haan, D. Burggraaf, J. Asjes, and R. Hille Ris Lambers. Background noise measurements for MEP-NSW Baseline TO. `http://www.noordzeewind.nl/wp-content/uploads/2012/02/OWEZ_R_251_T0_20070323_part_1_underwater_noise.pdf`. [Online PDF; accessed 05-JUN-2014].

[32] G. B. Hocker. Fiber optic acoustic sensors with composite structure: an analysis. *Appl. Opt.*, 18(21):3679–3683, 1979.

[33] F. Domingues, P. André, and M. Granada. Optical fibres coating aging indeced by the maritime environment. *Journal of Microwaves, Optoelectronics and Electromagnetic Applications*, 10(1):259–265, 2011.

[34] S. S. Patrick et. al. Responsivity and stability of air-backed, polycarbonate mandrel based fiber optic hydrophones. *Naval research laboratory*, 1993.

[35] Clay K Kirkendall and Anthony Dandridge. Overview of high performance fibre-optic sensing. *Journal of Physics D: Applied Physics*, 37(18):R197, 2004.

[36] Jens M. Hovem. *Marine Acoustics - The Physics of Sound in Underwater Environments*. Peninsula Publishing, first edition, 2012. ISBN 978-0-932146-65-6.

[37] Engineering.com. Generalized Hooke's Law. `http://www.engineering.com/Library/ArticlesPage/tabid/85/ArticleID/208/Generalized-Hookes-Law.aspx`. [Webpage; accessed 20-MAY-2014].

[38] G.B. Hocker. Fiber-optic sensing of pressure and temperature. *Appl. Opt*, 18: 1445–1448, 1979.

[39] Crystran. Silica Glass (SiO2) Data Sheet. `http://www.crystran.co.uk/userfiles/files/silica-glass-sio2-data-sheet.pdf`. [Online PDF; accessed 14-MAY-2014].

[40] Manuel Silva-López, Amanda Fender, William N. MacPherson, James S. Barton, Julian D. C. Jones, Donghui Zhao, Helen Dobb, David J. Webb, Lin Zhang, and Ian Bennion. Strain and temperature sensitivity of a single-mode polymer optical fiber. *Opt. Lett.*, 30(23):3129–3131, 2005.

[41] Roy M. Waxler, Deane Horowitz, and Albert Feldman. Optical and physical parameters of plexiglas 55 and lexan. *Appl. Opt.*, 18(1):101–104, 1979.

[42] Goodfellow. Polymethylmethacrylate - Material information. `http://www.goodfellow.com/E/Polymethylmethacrylate.html`, . [Webpage; accessed 01-JUN-2014].

[43] Ian P. Johnson, David J. Webb, and Kyriacos Kalli. Hydrostatic pressure sensing using a polymer optical fibre bragg gratings. *Proc. SPIE*, 8351:835106–835106–7, 2012.

[44] Goodfellow. Nylon-6 - Material information. `http://www.goodfellow.com/E/Polyamide-Nylon-6.html`, . [Webpage; accessed 01-JUN-2014].

[45] Goodfellow. Polycarbonate - Material information. `http://www.goodfellow.com/E/Polycarbonate.html`, . [Webpage; accessed 01-JUN-2014].

[46] MIT. Course - Mechanics of materials - Materials list. `http://ocw.mit.edu/courses/materials-science-and-engineering/3-11-mechanics-of-materials-fall-1999/modules/props.pdf`. [Online PDF; accessed 01-JUN-2014].

[47] Engineering toolbox. Bulk modulus of metals. `http://www.engineeringtoolbox.com/bulk-modulus-metals-d_1351.html`. [Webpage; accessed 01-JUN-2014].

[48] Prashil M. Junghare, Cyril Prasanna Raj P, T. Srinivas, and Preeta Sharan. A finite element analysis of fiber optic acoustic sensing mandrel for acoustic pressure with increased sensitivity. *American Journal of Engineering Research*, 02(09):01–07, 2013.

[49] A. Dandridge, A.B. Tveten, and T.G. Giallorenzi. Homodyne demodulation scheme for fiber optic sensors using phase generated carrier. *Microwave Theory and Techniques, IEEE Transactions on*, 30(10):1635–1641, 1982.

[50] Y. Léguillon, K. Hey Tow, P. Besnard, A. Mugnier, D. Pureur, and M. Doisy. First demonstration of a 12 dfb fiber laser array on a 100 ghz itu grid, for underwater acoustic sensing application. *Proc. SPIE*, 8439:84390J–84390J–8, 2012.

[51] FibroLAN. MDDX81 E 8 ITU Grid Channels DWDM devices . `http://www.fibrolan.com/FibroLAN/SendFile.asp?DBID=1&LNGID=1&GID=3460`. [Online PDF; accessed 05-JUN-2014].

[52] Thorlabs. PRO8 DWDM DFB Laser Diode Modules. `http://www.thorlabs.de/newgrouppage9.cfm?objectgroup_id=963`, . [Webpage; accessed 12-FEB-2014].

Appendix A

A

A.1 Calculation of mandrel sensitivity

```
% Calculation of sensitivity of mandrel

clear all;
close all;

% Silica fiber
n = 1.45; % Refractive index of fiber
v_1 = 0.17; % Poissons ratio of fiber

% Electrooptic coefficients
p_11 = 0.12;
p_12 = 0.27;

% Strain optic correction factor
xi = 1 - 0.5*n^(2) * ((1 - v_1)*p_12 - v_1*p_11);



E = 210e9; % Youngs modulus of mandrel
v_2 = 0.29; % Poissons ratio of inner tube
K = 160e9%E/(3*(1 - 2*v_2));

s = 20*log10((xi/(3*K))/10^6); % Sensitivity
```

A.2 Calculation of hollow mandrel sensitivity

```
% Calculation of sensitivity of hollow mandrel

clear all;
close all;

% Silica fiber
n = 1.45; % Refractive index of fiber
v_1 = 0.17; % Poissons ratio of fiber

% Electrooptic coefficients
p_11 = 0.12;
p_12 = 0.27;

% Strain optic correction factor
xi = 1 - 0.5*n^(2) * ((1 - v_1)*p_12 - v_1*p_11);


r = 50e-3; % Radius of cylinder
t = r/20; % Thickness of cylinder
E = 210e9; % Youngs modulus of tube
v_2 = 0.29; % Poissons ratio of inner tube

s = 20*log10( (((xi*r)/(E*t)) * (1-(v_2/2)))/10^(6)  );  Sensitivity
```